PIANC AUSTRALIA & NEW ZEALAND

PIANC AU-NZ Northern Chapter (Qld/NT)

Recent Developments in Design of Breakwaters

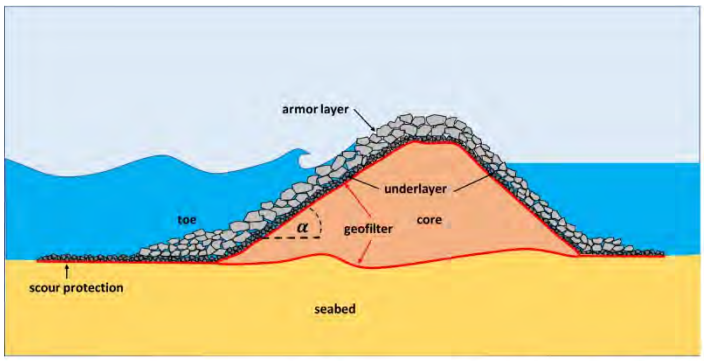

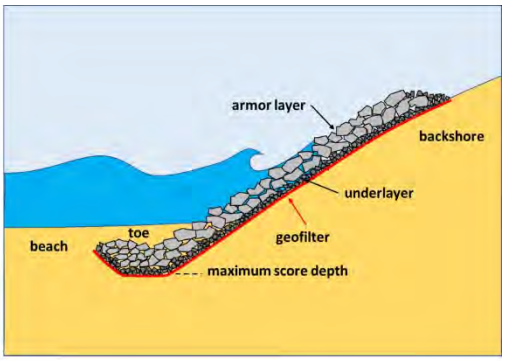

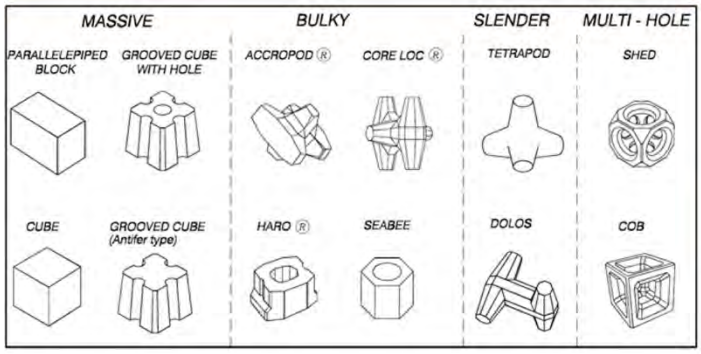

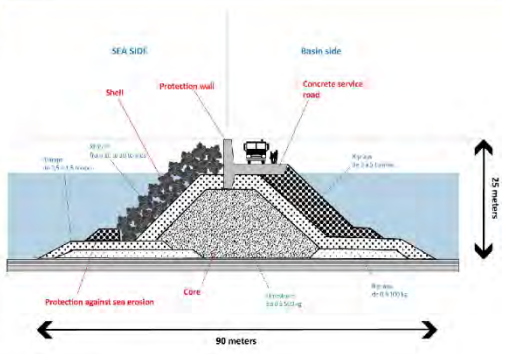

Griffith University – Gold Coast Campus - Map

PIANC AU-NZ Northern Chapter (Qld/NT)

Date:
03 June 2024 14:00 – 17:30

Arrival Time:
14:00 hrs

Event Start Time:
14:30 hrs

Venue:
Science, Engineering & Architecture Building (G39)
Hybrid Standard Lecture Theatre (1.17)
Griffith University, Gold Coast

Registration Options and Cost:

1. In person technical presentation with lab visit and networking drinks
    - PIANC Members - Free
    - Non-members - $30
2. Students (limited number) - Free

Register via trybooking link or with the below QR code.

This event is open to all PIANC Members and non-members. Not a member? Join us now! It's easy.

The PIANC ANZ Northern Chapter and Griffith University invites members and non-members to attend a technical session and networking event at Griffith University Gold Coast Campus. Hear from the academics and industry specialists on *"Recent Developments in Design of Breakwaters"* followed by Engineering Lab visit and networking drinks. Places are strictly limited; registrations are essential via trybooking to secure your place.

For more information and any questions, please contact:

Hari Panchumarthi (Hari.Panchumarthi@jacobs.com) or

Jasvinder Pantlia (Jasvinder.Pantlia@arup.com)

Welcome by Sam Mazaheri, Northern Chapter Chair PIANC ANZ

Welcome by Amir Etemad Shahidi, Senior Lecturer Griffith University Gold Coast

Recent Developments in the Design of Conventional Rubble Mound Structures by Amir Etemad Shahidi, Senior Lecturer Griffith University Gold Coast

Two-class Armor Berm Breakwaters – How to Design by Mohammed Al-Ogaili, PhD candidate at Griffith University, Coastal Engineering

Ecological Enhancement of Rock Structures – Working with Nature by Rick Plain, Senior Coastal and Maritime Engineer at Royal HaskoningDHV

Engineering Lab Visit at G09 building, 1.40 room

Networking drinks and nibbles after the lab visit

RECENT DEVELOPMENTS IN THE DESIGN OF CONVENTIONAL RUBBLE MOUND STRUCTURES

Amir Etemad-Shahidi

School of Engineering and Built Environment,
Griffith University

PIANC QLD/NT

2024, Gold Coast

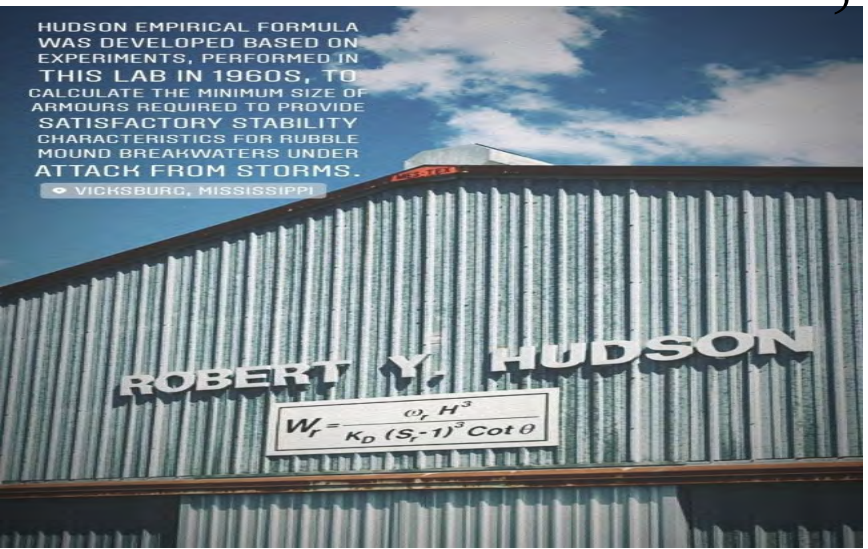

Acknowledgements:

Prof Marcel R.A. van Ge
TU Delft & Deltares
Co-author

Dr Meysam bali
PTP consulting Company

Dr Ali Koosheh
City of Moreton Bay

Outline:

- Introduction and motivation
- Mean overtopping discharge
- Slope stability
- Take home messages

Introduction

- Rubble mound structures such as breakwaters, seawalls, and revetments are the most common type of coastal structures.
- They are used to protect harbor basin and hinterland from the wave action.
- Two aspects need to be considered in their design: *safety and stability*.

Mean Overtopping Discharge

- The safety of rubble mound structures is mainly determined by the mean overtopping discharge.
- Excessive overtopping may result in damage to properties/structure and hazard to people.
- The crest level is usually determined based on the allowable mean overtopping discharge.

Wave Overtopping

Governing parameters

$q = f$ (wave characteristics and structure geometry)

q = (mean) overtopping discharge

H = wave height

T = wave period

β = angle of incident waves

Ru = runup

R_c = freeboard

tan α = slope of the structure and

γ_f = surface roughness (and porosity) factor

Overtopping (q)

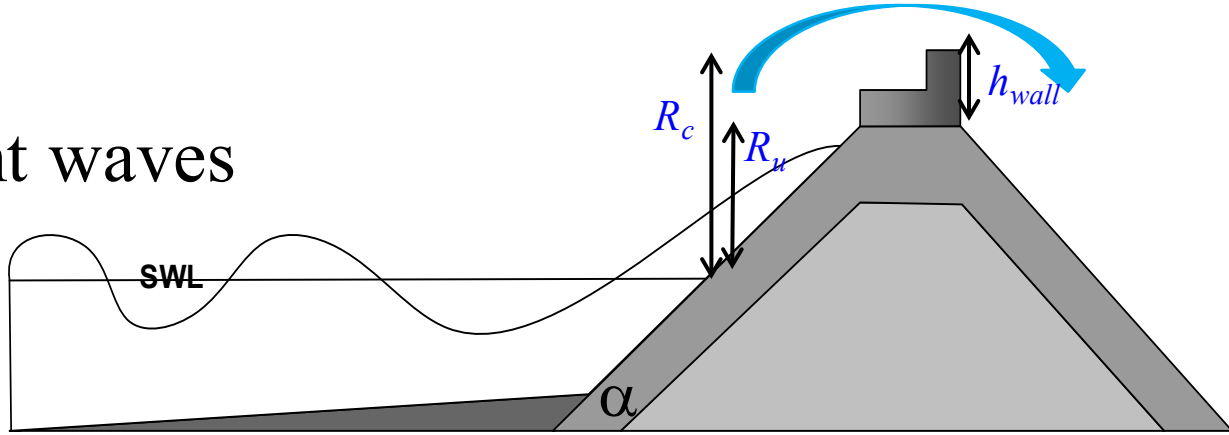

Existing formulas

Owen (1980):

$$Q^* = \frac{q}{gH_{m0}T_z} = a\exp\left(-b\frac{R_c}{H_{m0}}\sqrt{\frac{s_{oz}}{2\pi}}\frac{1}{\gamma_f}\right)$$

T_z = the mean zero crossing wave period,
H_{m0}= the (significant) spectral wave height
s_{oz} = the fictitious wave steepness (H_{m0}/L_{0z})
γ_f = roughness factor

EurOtop (2018) formula for $0.5 < \tan\alpha < 0.75$:

$$q^* = \frac{q}{\sqrt{g\cdot H_{m0}^3}} = 0.09\exp\left[-\left(1.5\frac{R_C}{H_{m0}\cdot\gamma_f}\right)^{1.3}\right]$$

Experiments

The original data set was the EurOtop 2018 database. It was enhanced by recent measurements of Koosheh et al. (2022).

EKV Formula

To derive a more physically-based formula, Etemad-Shahidi et al. (2022), correlated mean overtopping to runup as follows:

$$q^* = 1.22\times10^{-4} \exp\left[3.50\left(\frac{Ru_{2\%}-R_c}{H_{m0}}\right)\right] \quad \text{for } 0.25 < \tan\alpha < 0.8$$

Where runup is estimated using EurOtop (2018) formula:

$$R_{u2\%}/H_{m0} = 1.65\,\gamma_f\gamma_\beta\,Ir_{m\text{-}1,0} \le 1.0\,\gamma_{f\,surging}\gamma_\beta(4.0 - 1.5/\sqrt{Ir_{m\text{-}1,0}})$$

$$\gamma_{f\,surging} = \gamma_f + (Ir_{m\text{-}1,0}\text{-}1.8)\times(1-\gamma_f)/8.2 \ge \gamma_f$$

with a maximum of $R_{u2\%}/H_{m0} = 3$ (2) for impermeable (permeable) structures.

Scatter plot of mean overtopping rate, EurOtop and EKV formulas.

EurOtop (2018)

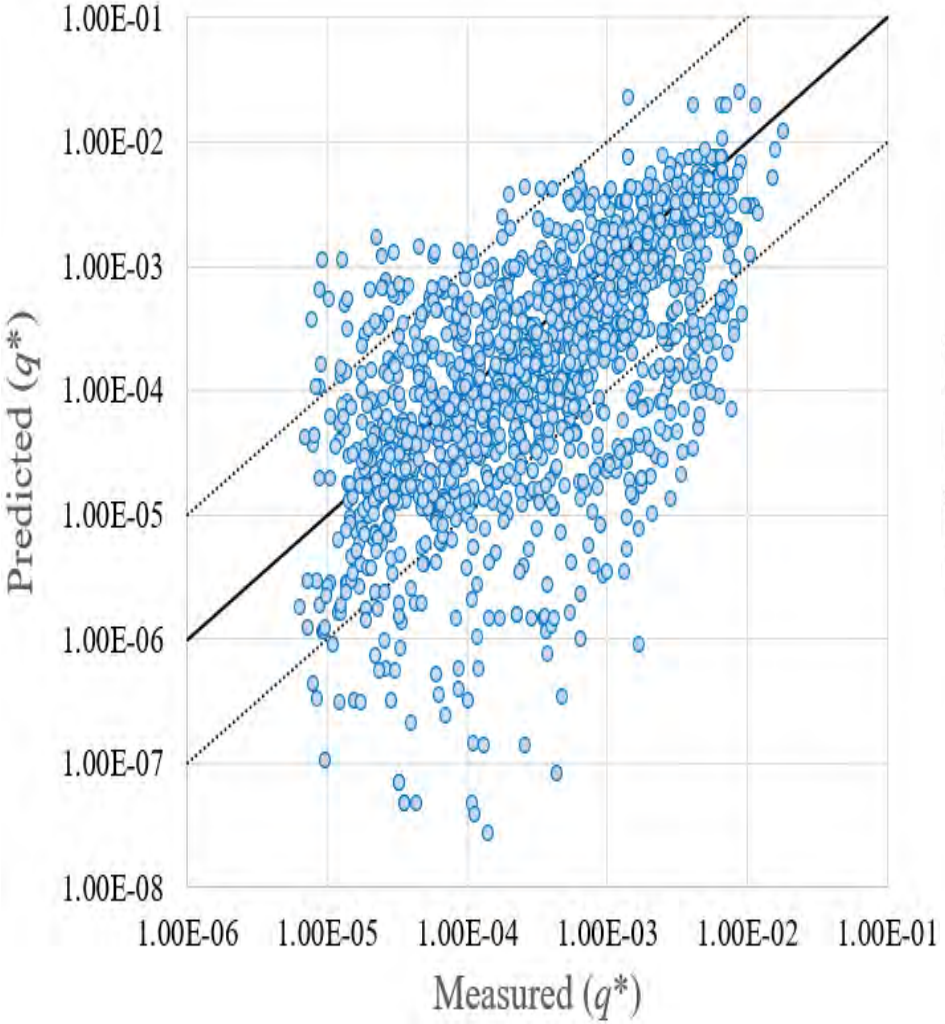

EKV (2022)

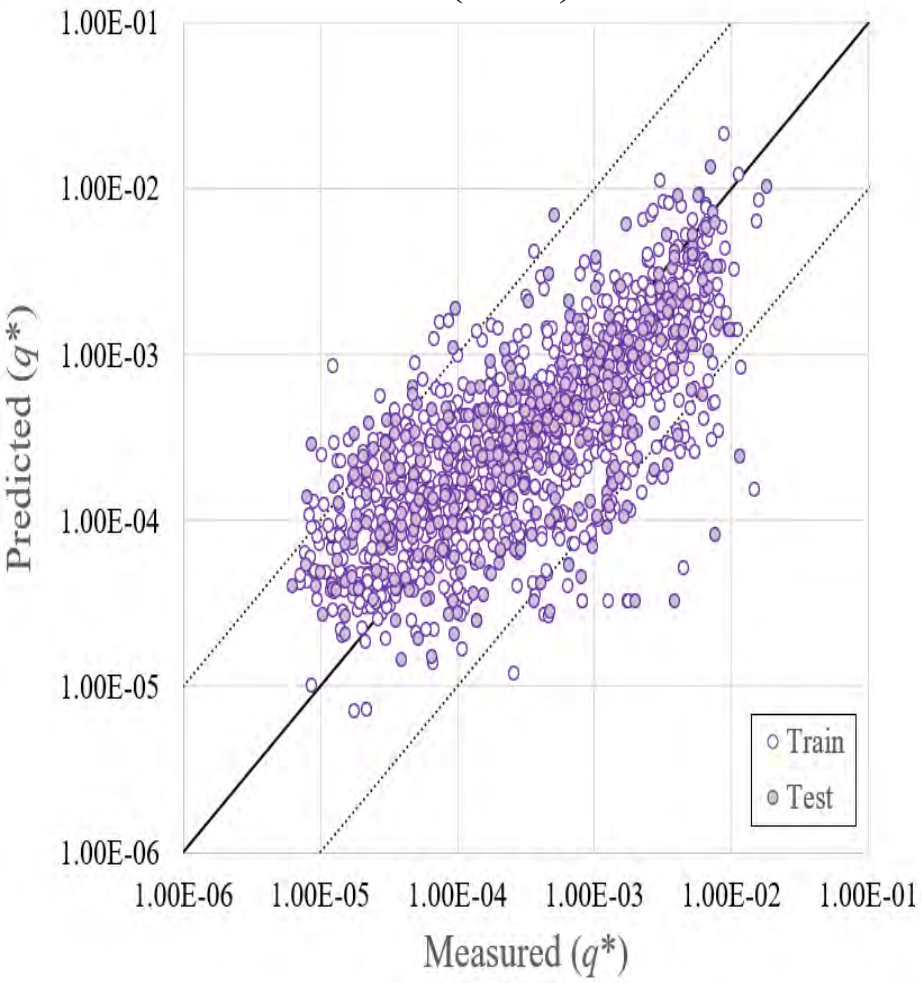

Evaluation of formulas

The following accuracy metrics were used to evaluate the performance of formulas:

$$BIAS = \frac{1}{n}\sum_{i=1}^{n}(\log P_i - \log M_i) \quad \text{and} \quad RMSE = \sqrt{\frac{1}{n}\sum_{i=1}^{n}(\log P_i - \log M_i)^2}$$

where M_i and P_i are the measured and predicted values, respectively; and n is the number of the records.

Accuracy metrics of different formulas, small-scale head on tests

Formula	*BIAS*	*RMSE*
Owen (1980)	0.26	0.74
EurOtop (2018)	-0.60	0.98
EKV (2022)	**0.00**	**0.54**

Slope stability: VdM formula

Van der Meer (1988) conducted tests using irregular waves and suggested the following:

$N_s = H_s/(\Delta D_{n50}) = 6.2\, S_d^{0.2} P^{0.18} N_w^{-0.1} Ir_m^{-0.5}$ for $Ir_m < Ir_{mc}$ (plunging)

$N_s = H_s/(\Delta D_{n50}) = S_d^{0.2} P^{-0.13} N_w^{-0.1} Ir_m^{P} cot\,\alpha^{0.5}$ for $Ir_m > Ir_{mc}$ (surging)

Where D_{n50} = the nominal rock median size, α = the structure front angle, = ρ_a/ρ_w-1 is relative buoyant density, S_d = the damage level and $Ir_{mc} = (6.2\, P^{0.31} \tan \alpha^{0.5})^{1/(P+0.5)}$.

P is the nominal permeability factor ranging from 0.1 to 0.6 and N_w is number of waves (storm duration).

The formula is only valid in *deep water* ($h/H_s > 3$). In addition, for P=0.5, the stability becomes independent of slope in surging (most common) conditions.

Etemad-Shahidi et al. (2020) formula

To overcome the limitations of VdM formula, Etemad-Shahidi et al. (2020), using a wide range of data, suggested the following:

$$N_s = 3.9 C_p N_w^{-1/10} S_d^{1/6} Ir_{m\text{-}1,0}^{-1/3} \quad \text{for } Ir_{m\text{-}1,0} \geq 1.8 \text{ (surging waves)}$$

$$N_s = 4.5 C_p N_w^{-1/10} S_d^{1/6} Ir_{m\text{-}1,0}^{-7/12} \quad \text{for } Ir_{m\text{-}1,0} < 1.8 \text{ (plunging waves)}$$

Where C_p, the permeability coefficient, is $[1+ (D_{n50c}/D_{n50})^{3/10}]^{3/5}$ and D_{n50c} is the median nominal size of core.

The formula is valid for both *deep and shallow* water tests.

For shallow water ($h/H_s < 3$), a correction factor of 1-3 m, where m is the foreshore slope, was suggested.

Evaluation of formulas

Accuracy metrics of formulas, small scale tests with $2 < S_d < 12$

Formula	*BIAS*	*RMSE*	*CC*
VdM (1988)	0.04	0.28	0.87
EBV (2020)	0	0.23	0.92

Take home messages

- Physically-based formulas improve prediction accuracy and are easier to comprehend.
- One important thing that practitioners need to consider is the uncertainty (due to data scatter) in the used equations.
- The given eqs for stability, say VdM does not include any safety factor and practitioners need to be aware of that.
- The adopted design approach, especially if physical modeling is not conducted, should be semi-probabilistic with a partial safety factor.

Thank for your attention

Effects of wave obliquity and spreading

Wave obliquity and directional spreading influence the stability

The following reduction factor (for rock size), has been suggested by Bali et al. (2023):

$$\gamma_\beta = (1\text{-}c_\beta)\cos^2\beta + c_\beta \quad \text{where } c_\beta = 0.44 + 0.004\,S$$

This means that c_β varies linearly between 0.44 for $S = 0$ (long crest waves) to 0.6 for $S = 40$ (short crested waves). In other words, the more the wave directional spreading, the less the effect of wave obliquity and the rock size can be reduced up to ~ 50% in very oblique waves.

Royal HaskoningDHV
Enhancing Society Together

Ecological Enhancement of Rock Structures – Working with Nature

Rick Plain – Coastal and Maritime Engineer

3rd June 2024

Working with Nature

- Nature Based Solutions
- Environmentally Sensitive Design / Environmentally Sustainable Design
- Eco Design / Eco Engineering
- ‘We do not inherit the Earth from our ancestors, we borrow it from our children’

New Concept?

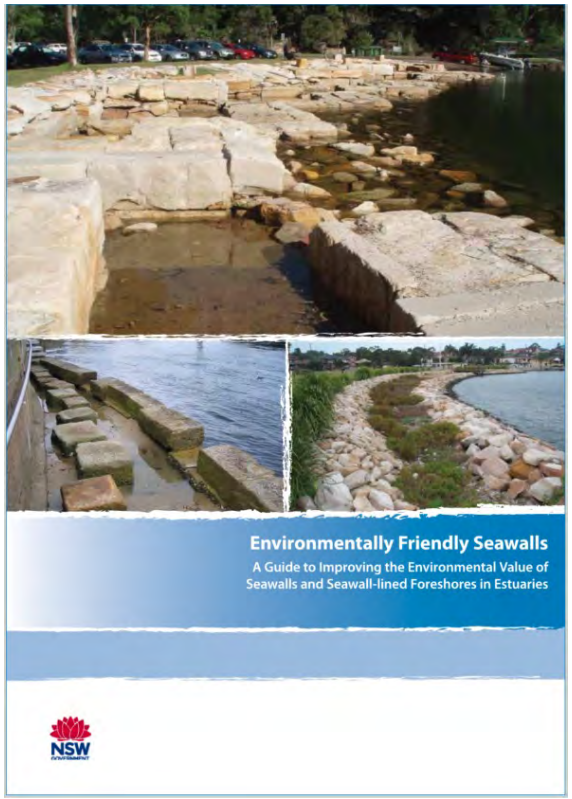
Environmentally Friendly Seawalls
A Guide to Improving the Environmental Value of Seawalls and Seawall-lined Foreshores in Estuaries
NSW

Why now?

- European Union introduced the **Corporate Sustainability Reporting Directive** in April 2021, which requires companies to prepare non-financial risk reports. The three main reporting areas are environmental, social and governance (ESG).
- The Australian Accounting Standards Board (AASB) released draft **Australian Sustainability Reporting Standards** in 2023.
- Australian Treasury released the Exposure Draft Treasury Laws Amendment Bill 2024: **Climate-related financial disclosure** (Exposure Draft legislation) (March).
- Commencing FY2025, companies will be obligated to disclose their sustainability metrics, encompassing actions to diminish greenhouse gas emissions, embrace renewable energy sources, and integrate sustainable practices across their operations.

Considerations

- Habitat creation
  - **Submerged/aquatic**
  - **Intertidal**
  - Terrestrial
- Whole-of-Life environmental impact (end of life).
- Carbon accounting / CO_2 emissions.
- Blue Carbon.

- Concrete emits ~620kg CO_2 per tonne. Concrete is responsible for ~8% of global CO_2 emissions.
- Seagrass, mangroves and saltmarsh occupy 2% of the seabed area but are responsible for 50% of the carbon captured and stored in the sediment (CSIRO).

Submerged / Intertidal Considerations

- Substrate, composition, surface texture, features and microhabitats
  - Sydney Harbour:
    - Concrete seawalls do not support the same diversity of species as sandstone seawalls (Connell and Glasby 1999; Moreira 2006) (high pH).
    - Introduced marine species in Sydney Harbour have colonised concrete surfaces in greater numbers than have native species yet the opposite is the case for natural reefs (Glasby et al. 2007).
- Size and slope

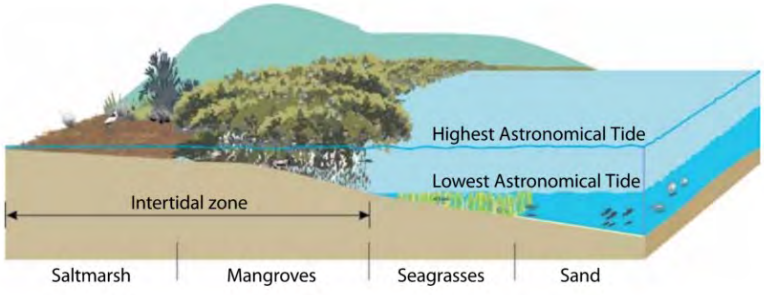

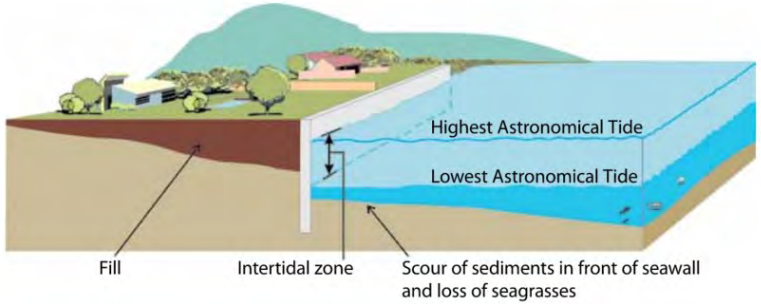

Terrestrial Considerations

- Separate fauna features from pedestrian areas.
- Predator barriers if necessary.
- Rookery crevices for birds and osprey towers/roosting features.
- Minimise artificial lighting, but if necessary, use shielding to reduce light pollution.
- Bury hard engineering structures with natural materials.
- Create pocket planting sites and improve soil properties for endemic coastal plant species.

Osprey at Richmond River (DPI, 2021)

Osprey tower for nesting (DPI, 2021)

Rock Breakwaters

- Breakwater maintenance and upgrades: multi-use and eco-features - guidance for asset owners, designers and project managers (DPI, 2021).
  - Armour (5 to 8 tonnes can be ideal) — to create crevices, overhangs and swim-throughs.
  - Install rock at the base of the structure to form a convoluted toe that maximises the habitat rich sand rock edge – use endemic (natural) rock.
  - Install detached structures to create gullies or embayments.
  - Eco-friendly concrete mixes with suitable texture (pH too high).

Convoluted Toe

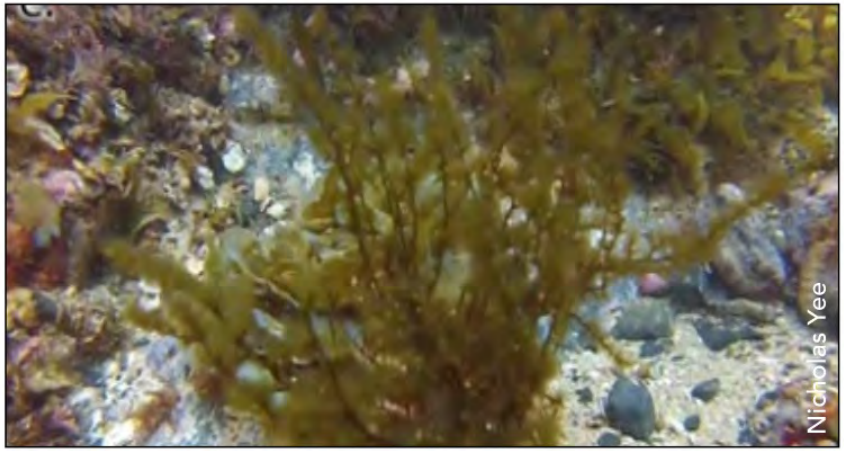

- Coffs Harbour North Breakwater (GHD)
  - Maximise the sand–rock interface area used by the critically endangered marine alga Nereia lophocladia
  - A 500 mm thick scree of greywacke cobble (sizes 100 – 250 mm and ~10% ~400 mm) extending 2-5m from the toe of the breakwater.

Submerged Breakwaters

Narrowneck Reef 16 months after placement – seagrasses, sponges, algae, fish assemblages.

Palm Beach Shoreline Protection Structure 26 months after placement. Complex habitat.

Vegetated Berms

‘With sea level rise, the saltmarsh will die’
‘Fish will become trapped behind the berm’

Vegetated Berms

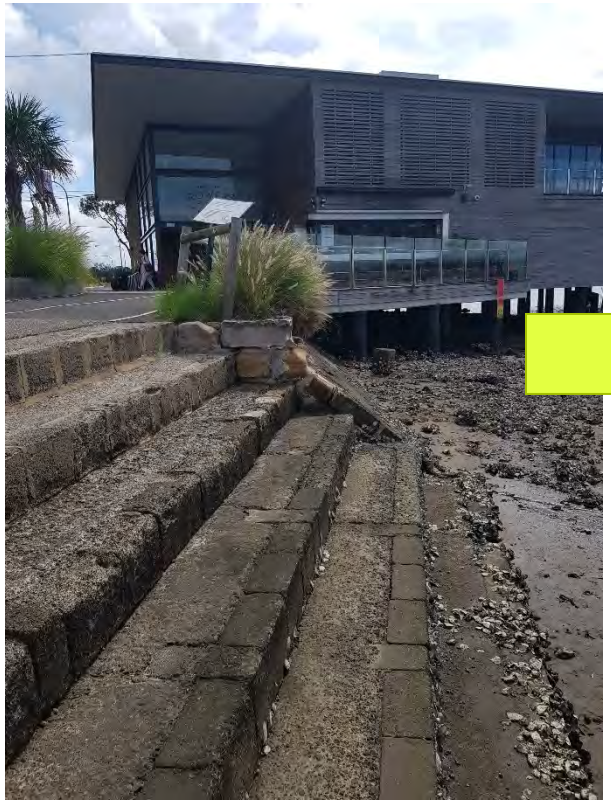

Intertidal Rock Pools

Reef Balls

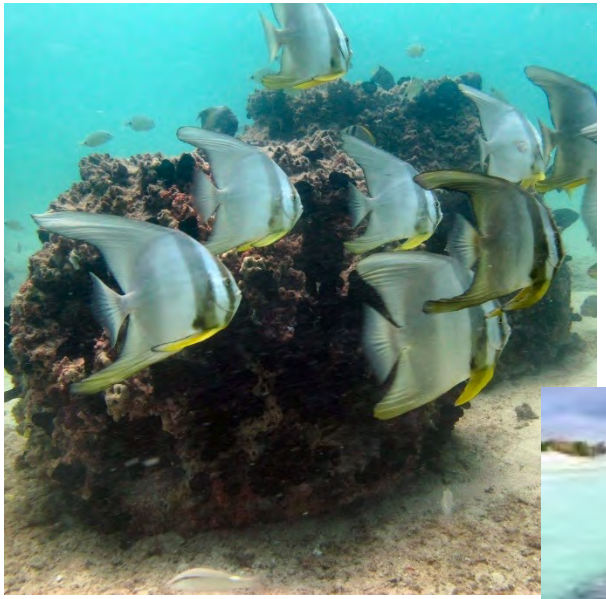

Reduced pH concrete with textured surface.

Catchment Solutions

Reduced pH concrete with textured surface.

Royal HaskoningDHV

SIMS Living Seawalls

ECOncrete

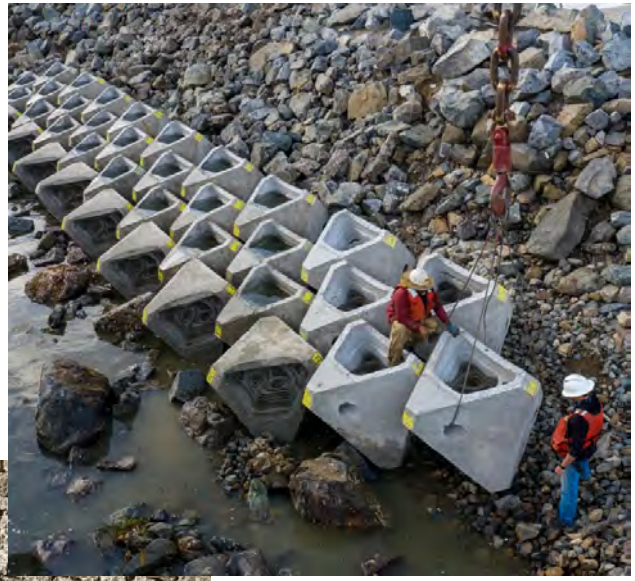

1. Concrete chemical composition.
2. Roughness and surface texture.
3. Shape.

Queensland Impediments

- State code 8: Coastal development and tidal works
  - PO17 Development is designed and sited to:
    1. avoid impacts on matters of state environmental significance; **or**
    2. **minimise** and mitigate impacts on matters of state environmental significance after demonstrating avoidance is not reasonably possible; **and**
    3. provide an offset if, after demonstrating all reasonable avoidance, minimisation and mitigation measures are undertaken, the development results in an acceptable significant residual impact on a matter of state environmental significance.
- State code 11: Removal, destruction or damage of marine plants
- State code 12: Development in a declared fish habitat area

- Marine Parks approvals.

*Marine plants are a matter of state environmental significance

Question Time

We all have a role to play!!

Coastal Engineering 193 (2024) 104576

Contents lists available at ScienceDirect

Coastal Engineering

journal homepage: www.elsevier.com/locate/coastaleng

Stability of two-class armour berm breakwaters: An experimental study

Mohammed Al-Ogaili [a], Amir Etemad-Shahidi [a,b,*], Nick Cartwright [a], Sigurdur Sigurdarson [c]

[a] School of Engineering and Built Environment, Griffith University, Southport, QLD, 4222, Australia
[b] School of Engineering, Edith Cowan University, WA, 6027, Australia
[c] IceBreak Consulting Engineers and Icelandic Road and Coastal Administration, Iceland

ARTICLE INFO

Keywords:
Recession
Erosion depth
Empirical formula
Berm breakwater
Design

ABSTRACT

The recession of a berm breakwater is a key parameter in ensuring its stability, and functionality, to protect coastal areas against wave impacts. Consequently, consideration of the expected recession in structural design is required to ensure the required objectives of the structure. In this study, physical model laboratory experiments were conducted to measure the recession of two-class armour berm breakwaters in response to varying sea state conditions (wave height, wave period, storm duration, and water depth at the structure's toe) and geometrical parameters (berm elevation from still water level, berm width, and rock size). A total of 110 tests were conducted under irregular wave forcing and the results were compared with those of existing formulae, derived specifically for mass armour and Icelandic-type berm breakwaters. Of the existing formulae, the Sigurdarson and Van der Meer (2013) formula that is derived for both mass armour and Icelandic-type berm breakwater outperforms the other formulas. Subsequently, a new empirical formula was developed to estimate the erosion depth based on the dimensionless water depth. The findings from this study could be instrumental for the structural design of two-class armour berm breakwaters under different sea states and geometrical configurations.

List of Symbols

α	Structure front slope angle
β	Mean wave direction
Δ	Relative buoyant density
ρ_s	Rock density (kg/m^3)
ρ_w	Water density (kg/m^3)
Ir_{op}	Iribarren based on peak period
A_e	Eroded area of the profile
b	Empirical fitted coefficient
$b1$	Correlation factor.
B	Berm width
cot α_d	The initial front slope below the berm
D_{n50}	The median nominal diameter of the armour
D_{n50l}	Median nominal diameter of the top armour
D_{15}	Sieve diameter exceeds by 85% of a sample
D_{85}	Sieve diameter exceeds by 15% of a sample
D_{n15}	Nominal diameter, or equivalent cube size, (by weight) $Dn15 = (W_{15}/\rho_s)^{1/3}$
D_{n85}	Nominal diameter, or equivalent cube size, (by weight) $Dn85 = (W85/\rho_s)^{1/3}$
DR	Discrepancy Ratio (predicted value divided by measured value)
f_g	Gradation of stone material
$f_{grading}$	Factor accounting for the effect of stone gradation
f_N	Factor accounting for the effect of number of waves

(*continued on next column*)

(*continued*)

f_β	Factor accounting of the influence of wave direction
$f_{skewness}$	Factor considering the influence of wave skewness
FR	Fully Reshaping berm breakwater
g	Acceleration due to gravity
G_c	Crest width
h	Water depth at the toe of the structure
h_{br}	Berm elevation above SWL (negative if berm is above SWL)
h_f	Erosion depth
h_I	thickness of Armour layer 1 (m)
h_s	Water depth above the step
H_0	Stability number, H_0=H_s/ ΔD_{n50}
H_{mo}	Significant wave height based on frequency domain analysis
H_s	Significant wave height or $H_{1/3}$
H_{sD}	100-year design wave height
HR	Hardly Reshaping berm breakwaters
L_{op}	Deep water wavelength based on peak period
N_w	Number of waves (Test duration/$T_{0,1}$)
O_i	Measured value
PR	Partly Reshaping berm breakwater.
P_i	Predicted value
R_C	Crest freeboard
Rec	Recession of the berm

(*continued on next page*)

* Corresponding author. School of Engineering and Built Environment, Griffith University, Southport, QLD, 4222, Australia.
E-mail address: a.etemadshahidi@griffith.edu.au (A. Etemad-Shahidi).

https://doi.org/10.1016/j.coastaleng.2024.104576
Received 3 April 2024; Received in revised form 7 July 2024; Accepted 8 July 2024
Available online 10 July 2024

(*continued*)

Rec_{av}	The Recession of the average profiles (averaged between the water level and the top of the berm)
R_e	Reynolds number
N_{sn}	Stability dimensionless parameter
MSE	Mean Square Error $= \frac{1}{N}\sum_{i=1}^{N}(P_i - O_i)^2$
NBIAS	Normalized bias $= \frac{\frac{1}{N}\sum_{i=1}^{N}(P_i - O_i)}{\frac{1}{N}\sum_{i=1}^{N}O_i} \times 100$
Sc	Threshold value of the recession
SI	Scatter index $= \frac{\sqrt{\frac{1}{N}\sum_{i=1}^{N}(P_i - O_i)^2}}{\frac{1}{N}\sum_{i=1}^{N}O_i} \times 100$
S_d	Damage parameter
s_{0m}	Deep water wave steepness based on mean wave period $T_{0,1}$
s_{0p}	Deep water wave steepness based on peak period
SWL	Still Water Level
T_0	Dimensionless wave period $= \sqrt{g/D_{n50}}\ T_{0,1}$
T_{0p}	Peak wave period
T_m	Mean wave period
T_z	Mean zero up-crossing period
$T_{0,1}$	Spectral mean wave period
T_0^*	Dimensionless wave period transition point
W_{50}	Median Weight
W_{85}	Weight exceeded by 85% of a sample
W_{15}	Weight exceeded by 15% of a sample

1. Introduction

Berm breakwaters play a significant role in coastal protection due to their capacity to dissipate wave energy through the incorporation of a large porous berm located above the still water level. The berm breakwaters' large capability to dissipate wave energy can contribute to the stability. Moreover, berm breakwaters offer a better use of quarry yield and available construction equipment and more importantly the maintenance cost and overall stability (Sigurdarson et al., 1999). Berm breakwaters can be broadly classified into two main types: mass armoured (Fig. 1a) and the Icelandic-type (Fig. 1b). Mass armour berm breakwaters are characterized by a single grading of armour rock. In contrast, the Icelandic-type breakwater comprises several classes of rocks within its armour layer. Generally, the armour layers of the Icelandic-type consist of narrow gradations that lead to higher permeability, facilitating efficient wave energy absorption and overall structural stability. The behaviour of both types is different as a relatively small rock is used for the mass armoured berm breakwater compared to a large rock for the Icelandic-type berm breakwater especially in the top layers. The significant advantage of the Icelandic-type is its excellent stability which is achieved by sorting the quarry rocks into several classes laying the larger rock in the upper part of the berm. However, this procedure required a more complicated construction method.

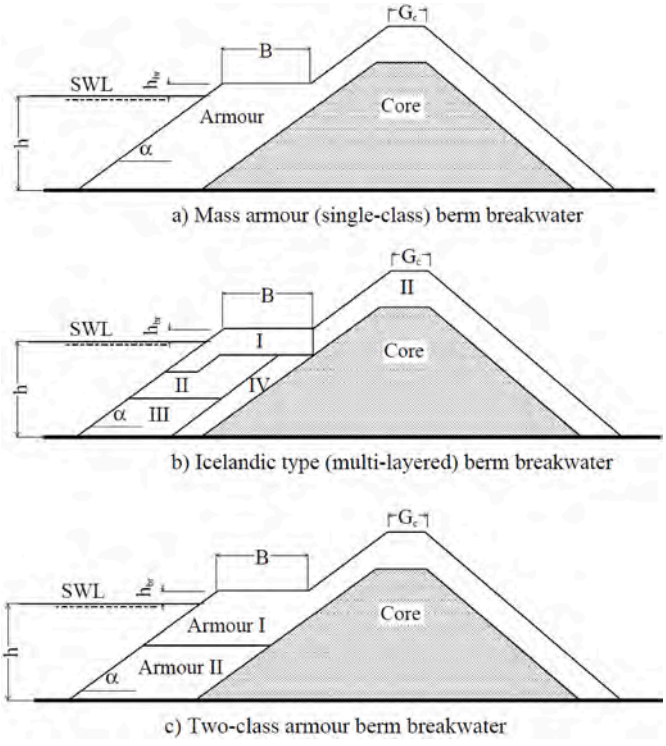

Fig. 1. Schematic cross section of a) Mass armour (MA) berm breakwater b) Icelandic-type (IC) berm breakwater c) Two-class armour berm breakwater (Al-Ogaili et al., 2022).

Therefore, combining the above two types of berm breakwaters could be a way to achieve the advantages the simplicity in constructions from the mass armour and the great stability of the Icelandic-type. The reduction in the number of stone classes in the underlying layers has an insignificant impact on the stability as they are less exposed to wave action. A two-class armour berm breakwater is more stable than mass armour ones (with the same D_{n50}). In addition, this composition will reduce the complexity, required time, and cost of construction compared to those of the Icelandic type. Van der Meer and Sigurdarson, (2016) mentioned that splitting the wide graded single class mass armour berm into two narrower graded armour classes (Fig. 1c) could improve the stability at a lower cost, and earlier Juhl and Sloth (1998) found out that adding an armour layer at the top of the mass armour type berm breakwaters will reduce the berm recession. In this layer composition, the determination of the thickness of the top layer is essential for structural stability as a thinner top layer may lead to erosion of the bottom weaker layer and hence a collapse.

Several formulas have been developed to estimate the stability of the mass armour and Icelandic-type berm breakwaters and most of them have examined the berm recession (Fig. 2), which is the most important parameter for the stability of the berm breakwaters. However, the stability and the hydraulic response of two–class armour berm breakwater have not been studied yet. Lately Al-Ogaili et al. (2022) examined existing stability formulas and noticed that there is no agreement among them regarding the effect of some geometrical and hydraulic parameters such as the berm width, storm duration and wave period.

Accurate prediction of the recession is essential to ensure the breakwater's performance and to optimize construction costs. Using the existing formulae developed for mass armour and Icelandic-type berm breakwaters might be inappropriate and results in unstable or costly designs. Hence, there is a necessity to investigate the stability of the two-class armour berm breakwater to identify the role of different parameters such as wave height, wave period, and layer thickness.

This study aims to provide tools for the design of two-class armour berm breakwaters. The specific objectives are: (a) investigating the stability of the two-class armour berm breakwaters under different wave conditions, (b) evaluating the performance of existing formulas to predict the recession of two-class armour berm breakwater, and (c) providing a formula to estimate the erosion depth and hence the thickness and depth of the top layer. Erosion depth (h_f) is the distance between the SWL, and the intersection point between the initial and the "S"-shaped profiles (Fig. 2). To achieve these, 110 experiments were conducted exclusively on two-class armour berm breakwater. Most of the tests represented all berm breakwaters classes with a wide range of parameters.

2. Background

Berm breakwaters are classified based on two factors: the deformation levels and construction methods. Sigurdarson and Van der Meer (2013) improved PIANC (2003) classifications and provided design ranges and expected recession for different types of berm breakwaters

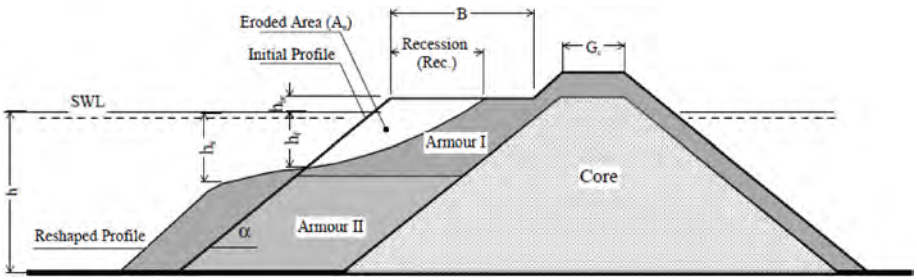

Fig. 2. Initial and reshaped profiles of the Two-class armour berm breakwater.

Table 1
Classification of berm breakwaters (Sigurdarson and Van der Meer, 2013).

	Abbreviation	$H_{sD}/\Delta.D_{n50}$	S_d	Rec/D_{n50}
Hardly reshaping Icelandic-type berm breakwater	HR-IC	1.7–2.0	2–8	0.5–2
Partly reshaping Icelandic-type berm breakwater	PR-IC	2.0–2.5	10–20	1–5
Partly reshaping mass armoured berm breakwater	PR-MA	2.0–2.5	10–20	1–5
Fully reshaping mass armoured berm breakwater	FR-MA	2.5–3.0	–	3–10

(Table 1).

where H_{sD} is the 100-year design wave height, Δ is the relative buoyant density given as $\frac{\rho_s-\rho_w}{\rho_w}$, ρ_s is the rock's density (kg/m^3), ρ_w is the water density (kg/m^3), D_{n50} is the median nominal diameter of the armour rock (m), S_d is the damage level, and *Rec* is the recession of the berm.

Van der Meer and Sigurdarson (2016) stated that the berm breakwaters should be statically stable with $H_s/\Delta D_{n50} \leq 3.0$. This is mainly because the dynamically stable structures are affected by longshore transport.

The design of berm breakwaters takes into consideration many factors like wave height, wave period, berm geometry, and erosion depth to ensure hydraulic stability. Empirical formulas are commonly used to predict the required dimensions and configuration. In addition to the recession, another important parameter is the erosion depth discussed below.

2.1. Berm recession

Many researchers have developed formulas to predict the berm recession such as Tørum (2007), Sigurdarson et al. (2008), Lykke Andersen and Burcharth (2010), Moghim et al. (2011), Shekari and Shafieefar (2013), and Sigurdarson and Van der Meer (2013).

Tørum (2007) revised Tørum et al. (2003) formula using data from both mass armour (MA) berm breakwaters and Icelandic (IC) ones. They provided a formula for the recession as a function of (H_0T_0), rock grading, and water depth effects as below:

$$\frac{Rec}{D_{n50}} = 0.0000027(H_0T_0)^3 + 0.000009(H_0T_0)^2 + 0.11(H_0T_0) - \left[f\left(f_g\right) + f\left(\frac{h}{D_{n50}}\right)\right]\frac{H_0T_0}{120} \quad (1)$$

Where H_0=$H_s/\Delta D_{n50}$ is the stability number and H_s is the significant wave height. $T_0 = \sqrt{g/D_{n50}}\,T_Z$ is the dimensionless wave period and T_Z is the mean zero up-crossing period. The gradation factor, $f\left(f_g\right)$ and the depth factor, $f\left(\frac{h}{D_{n50}}\right)$ are given as:

$$f\left(f_g\right) = -9.9f_g^{\,2} + 23.9f_g - 10.5 \quad \text{for } 1.3 < f_g < 1.8 \quad (2)$$

$$f\left(\frac{h}{D_{n50}}\right) = -0.16\,\frac{h}{D_{n50}} + 4.0 \quad \text{for } 12.5 < \frac{h}{D_{n50}} < 25 \quad (3)$$

where f_g=D_{n85}/D_{n15}. $D_{n85} = (W_{85}/\rho_s)^{1/3}$ is the nominal diameter, or equivalent cube size (by weight) and $D_{n15} = (W_{15}/\rho_s)^{1/3}$. W_{85} and W_{15} are the weight exceeded by 15% and 85% of a sample respectively. It is noteworthy that this equation is valid for H_0T_0 > 20-30.

Lykke Andersen (2006) and later Lykke Andersen and Burcharth (2010) conducted large numbers of tests on mass armour berm breakwaters with a wide range of parameters, i.e., stability numbers between 0.96 and 4.86, 16.8< H_0T_0 <163 and 0.01< s_{0p} <0.054.

They examined the effect of various parameters such as wave height and deep water mean wave steepness (s_{om}), berm width (B), berm height (h_{br}), crest freeboard (Rc), and water depth (h) and presented the following equations:

$$\frac{Rec}{D_{n50}} = f_{hbr}\left(f_{H0}\frac{2.2h - 1.2h_s}{h - h_{br}}f_\beta f_N f_{grding} f_{skewness} - \frac{(\cot(\alpha d) - 1.05)}{2D_{n50}}(h - h_{br})\right) \quad (4)$$

Where cot α_d is the inverse of initial front slope below the berm.

Where $f_{h_{br}}$ is the influence of the berm height factor given as:

$$f_{hbr} = \begin{cases} 1 \; for \; \dfrac{h_{br}}{H_{m0}} \leq 0.1 \\ 1.18\,exp\left(-1.64\dfrac{h_{br}}{H_{m0}}\right) for \; \dfrac{h_{br}}{H_{m0}} > 0.1 \end{cases} \quad (5)$$

Where H_{m0} is the significant wave height based on frequency domain analysis and

$$f_\beta = cos\,(\beta) \quad (6)$$

This factor accounts for the influence of wave direction and β is the mean wave direction.

$$f_{skewness} = exp\left(1.5b_1^{\,2}\right) \quad (7)$$

$f_{skewness}$ considers the influence of wave skewness and b_1 is a correlation factor used to estimate wave skewness.

$$f_N = \begin{cases} \left(\dfrac{N_w}{3000}\right)^{-0.046H_0+0.3} \quad for\ H_0<5 \\ \left(\dfrac{N_w}{3000}\right)^{0.07} \quad for\ H_0\geq 5 \end{cases} \quad (8)$$

where f_N is the actor accounting for the effect of number of waves and N_w is the number of waves. h_s, water depth above step (Fig. 2), is given as:

$$h_s = 0.65\,H_{m0}\,s_{0m}{}^{-0.3}f_N f_\beta \quad (9)$$

where, s_{0m} is the fictitious deep water wave steepness calculated as 2 π

$H_{m0}/g\ T_{0,1}{}^2$, and $T_{0,1}$ is the spectral mean wave period. $T_0{}^*$ is called the dimensionless wave period transition point given as:

$$T_0{}^* = \frac{19.8\ exp\left(-\frac{7.08}{H_0}\right) s_{0m}{}^{-0.5} - 10.5}{0.05\ H_0} \tag{10}$$

and

$$f_{H0} = \begin{cases} 19.8\ exp\left(-\frac{7.08}{H_0}\right) s_{0m}{}^{-0.5}\ for\ T_0 \geq T_0{}^* \\ 0.05 H_0 T_0 + 10.5\ for\ T_0 < T_0{}^* \end{cases} \tag{11}$$

where $T_0 = \sqrt{g/D_{n50}}\ T_{0,1}$ and

$$f_{grading} = \begin{cases} 1\ for\ f_g \leq 1.5 \\ 0.43 fg + 0.355\ for\ 1.5 < f_g < 2.5 \\ 1.43\ for\ f_g \geq 2.5 \end{cases} \tag{12}$$

$f_{garding}$ accounts for the effect of stone gradation.

Sigurdarson et al. (2008) refined the PIANC (2003) data by focusing on specific criteria to better represent the recession of Icelandic type of berm breakwaters (IC). They established limits such as the structure's cross-section, rock classification, and wave height measurement location to ensure the selected data sets were more reliable. They suggested the following formula which includes H_0T_0 parameter only:

$$\frac{Rec}{D_{n50}} = 0.032\left(H_0 T_{0p} - Sc\right)^{1.5} \tag{13}$$

$$\frac{Rec}{D_{n50}} = 0 \quad for\ H_0 T_{0p} < Sc \tag{14}$$

where $T_{0p} = \sqrt{g/D_{n50}}\ T_p$ and T_p is the peak wave period. Sc is the threshold of the recession with a mean value of 35 and standard deviation of 5, for $H_0 T_{0p} < 70$.

Moghim et al. (2011) studied the influence of berm width, berm height, wave height, wave period, number of waves, and the water depth; on the recession of mass armour berm breakwaters with H_0 between 1.58 and 3.9.

They proposed a new dimensionless parameter ($H_0\sqrt{T_0}$) to estimate the recession of MA berm breakwaters. Their formulae for the estimation of the recession are:

$$\frac{Rec}{D_{n50}} = \left(10.4\left(H_0\sqrt{T_{0p}}\right)^{0.14} - 13.6\right)\left(1.61 - exp\left(-2.2\left(\frac{N_w}{3000}\right)\right)\left(\frac{h_{br}}{H_s}\right)^{-0.2}\left(\frac{h}{D_{n50}}\right)^{0.56} for\ H_0\sqrt{T_{0p}} < 17\right) \tag{15}$$

$$\frac{Rec}{D_{n50}} = \left(0.089 H_0\sqrt{T_{0p}} + 0.49\right)\left(1.61 - exp\left(-2.2\left(\frac{N_w}{3000}\right)\right)\left(\frac{h_{br}}{H_s}\right)^{-0.2}\left(\frac{h}{D_{n50}}\right)^{0.56} \quad for\ H_0\sqrt{T_{0p}} \geq 17\right) \tag{16}$$

The above equations are valid for: $7.7 < H_0\sqrt{T_{0p}} < 24.4$, $500 < N_w < 6000$, $0.12 < \frac{h_{br}}{H_s} < 1.24$, $8 < \frac{h}{D_{n50}} < 16.5$, and $1.2 < f_g < 1.5$.

Shekari and Shafieefar (2013) also developed a formula for mass armour berm breakwaters similar to that of Moghim et al. (2011) but they added the effect of berm width as follows:

$$\frac{Rec}{D_{n50}} = \left(-0.016\left(H_0\sqrt{T_{0p}}\right)^2 + 1.59 H_0\sqrt{T_{0p}} - 9.86\right)\left(1.72 - exp\left(-2.19\frac{N_w}{3000}\right)\right)\left(\frac{h_{br}}{H_s}\right)^{-0.21}\left(\frac{B}{D_{n50}}\right)^{-0.15} \tag{17}$$

The limitations of the above equation are: $7.09 < H_0\sqrt{T_{0p}} < 23.52$, $500 < N_w < 6000$, $0.22 < \frac{h_{br}}{H_s} < 1.57$, $9.6 < \frac{h}{D_{n50}} < 14.11$ and $14 < \frac{B}{D_{n50}} < 29.41$.

Sigurdarson and Van der Meer (2013) and later Van der Meer and Sigurdarson (2016) collected data from several studies from both mass armour berm breakwater and Icelandic type of berm breakwaters (IC) and derived a simple formula to predict the recession of the berm breakwater.

$$\frac{Rec_{av}}{D_{n50}} = 1.6(H_0 - 1.0)^{2.5} \tag{18}$$

$$\frac{Rec_{av}}{D_{n50}} = 0\ for\ H_0 < 1.0 \tag{19}$$

They defined Rec_{av} as the recession of the average profiles (averaged between the water level and the top of the berm). It is noteworthy that the recession in Sigurdarson and Van der Meer (2013) formula depends mainly on the stability number; and the effect of slope angle, berm level, and toe depth are considered in an accompanying scoring table. They argued that different classes of berm breakwaters might respond differently to changes in the above mentioned geometrical parameters. Hence, assigning a numerical score or weight to each parameter was suggested to adjust their formula's prediction formula to better suit a specific class of berm breakwaters. More details regarding the formulas are provided in Appendix A.

2.2. Erosion depth (h_f)

The location of the intersection point (h_f) or the erosion depth is important for the design of the berm breakwaters because the depth of the top layer of the Icelandic-type and the two-class type armour berm breakwater needs to be located below this point to ensure that the lower layer, typically composed of smaller rocks, remains protected from direct wave action.

Sveinbjörnsson (2008) suggested that the depth of the top layer should be as follows:

$$\text{Thickness of Top layer} \geq 1.45\Delta D_{n50}\ \text{ Class I (Armour I)} \tag{20}$$

$$\text{Thickness of Top layer} \geq 1.85\Delta D_{n50}\ \text{Class II (Atmour II)} \tag{21}$$

Tørum et al. (2003) reported that reshaping profiles for different wave heights pass through the same point during the reshaping. In simpler terms, the erosion depth h_f is almost the same for different wave heights. By comparing the results of the experiments with different water depths, they proposed the following formula to relate h_f with water depth h:

$$\frac{h_f}{D_{n50}} = 0.2\frac{h}{D_{n50}} + 0.5 \quad For\ \ 10 < \frac{h}{D_{n50}} < 25 \tag{22}$$

where h is water depth at the toe of the structure (m).

Later Lykke Andersen et al. (2012) stated that the value of h_f was different from what obtained using the previous equation. They tested Tørum et al. (2003) formula for their experimental data and noticed that Eq. (22) underestimates the h_f in most of the tests. Hence, they slightly modified Tørum et al. (2003) formula by replacing the coefficient of 0.2 with 0.3 as shown below.

$$\frac{h_f}{D_{n50}} = 0.3\frac{h}{D_{n50}} + 0.5 \quad (23)$$

Later Moghim and Lykke Andersen (2015) evaluated the above formulas and found that they underestimated the erosion depth. They referred the reason to the range of their new tests which were different from that of Eq. (22), and proposed the following equation to reduce the bias:

$$\frac{h_f}{D_{n50}} = 0.18\frac{h}{D_{n50}} + 2.3 \quad (24)$$

Ehsani et al. (2020) recently derived a formula to estimate the erosion depth of the Icelandic-type berm breakwater. Furthermore, they noticed through their experiments that the erosion depth is partially influenced by the berm level above the water level. Therefore, they included the effect of the berm level as:

$$\frac{h_f}{D_{n50}} = 0.145\left(\frac{h}{D_{n50}}\right)^{1.332}\left(\frac{h_{br}}{D_{n50}}\right)^{-0.358} \quad (25)$$

where h_{br} is the berm elevation above SWL (negative if berm is above SWL).

Later, Van der Meer and Sigurdarson (2016) proposed that the transition from layer I to layer II below the water level should be 0.4 H_{sD} for the Icelandic-type and 0.6 H_{sD} for the two-class armour berm breakwaters.

To sum up, the literature indicates that the thickness of the top layer (armour 1) mostly depends on the water depth. To maintain the stability and the integrity of the two-class armour berm breakwater and safeguard the armour 2 layer, this thickness should be greater than the erosion depth.

3. Experimental set-up

The experiments were carried out in a 0.5 m wide, 0.8 m deep, and 22.5 m long wave flume at the hydraulics laboratory of Griffith University, Australia (Fig. 3). The flume is equipped with glass panels flume for easy monitoring and recording (Fig. 3).

A computer controlled; piston type wave maker is at one end of the flume which has a dynamic wave absorption system to minimize the wave re-reflection from the wave paddle. Irregular waves of the JONSWAP spectrum with a peak enhancement factor (γ) of 3.3 were used for all the tests. A summary of wave parameter ranges can be found in Table 2.

A group of three capacitance type wave gauges was placed near the toe of the structure to analyse the wave field according to the Mansard and Funke (1980) method to distinguish between the incident and reflected waves (Fig. 4). They suggested the following arrangement of the three gages: $X_{12} = L_{0p}/10$ and $L_{0p}/6 < X_{13} < L_{0p}/3$; where X_{12} and X_{13} are the distances of the second and third gauges from the first, respectively; and L_{0p} is the deep-water wavelength obtained using peak wave period. To reduce the effect of the waves reflected from the structure on the measured incident waves, the nearest wave gauge (WG3) was placed far enough ($X_3s > 0.4\ L_{0p}$) from the structure (Klopman and Van Der Meer, 1999).

Table 2
Ranges of measured parameters.

Parameters (unit)	Range	Parameters (unit)	Range
Wave height, H_s (m)	0.05–0.13	$H_{0_}$Armour layer 1	1.2–3.10
Peak wave period T_{op} (s)	1.1–2.0	$T_o = \sqrt{g/D_{n50}}\ T_{0,1}$	17.5–34.0
Water depth, h (m)	0.40–0.475	$H_0T_{0_}$Armour layer 1	23–95
Berm height h_{br} (m)	0.026–0.10	$H_0\sqrt{T_{0_}}$Armour layer 1	8.0–17
Berm width B (m)	0.165–0.282	h/D_{n50}	17.2–20.5
cot α	1.5	h/H_s	3.5–9.4
h_I thickness of Armour layer 1 (m)	0.12–0.20	h_{br}/H_s	0.2–1.2
Crest freeboard R_c (m)	0.08–0.20	R_c/H_s	0.70–2.2
Crest Width G_c (m)	0.12	s_{0p}	0.01–0.06
Rec/D_{n50}	0.85–12	h_f/H_{m0}	0.52–1.47
N_w (Test duration/$T_{0,1}$)	1000–4000	B/D_{n50}	7.1–12.2

The two-class armour berm breakwater was constructed at the end of the flume. The model consists of two classes of narrower-graded armour rocks (Al-Ogaili et al., 2022). The first armour layer was constructed with a D_{n50} of 0.023 m, the second armour layer with a D_{n50} of 0.017 m, and a permeable core with a D_{n50} < 0.013 m. A summary of the rock classes used in the experiments is shown in Table 3.

To minimize viscous scale effects, the Reynolds number (Re) of the tests should be high enough. Van der Meer (1988) stated that the lowest value of the Reynolds number with no scale effect, is 1.0×10^4. In this study, the Reynolds numbers of all tests were between 2×10^4 to 3×10^4, and hence the viscous scale effects are negligible.110 tests have been conducted with a wide range of tested parameters (Table 2) to study the influence of the sea state condition and structural parameters with about 1500 waves for each test. In addition, eight separate non-cumulative tests were conducted to investigate the influence of the number of waves (N_w).

Two-class armour berm breakwaters have characteristics similar to those of the mass armour ones. Therefore, they are mostly partly reshaped (PR) type structures. The focus of this study was also on the behaviour of the PR berm breakwaters which are more common in practice. Hence, from a total of 110 experiments; 25 tests examined the HR berm breakwaters, and 85 tests were on PR ones.

All experiments were conducted within the realistic range of parameters. For example, the maximum stability number (H_0) was set to ~ 3.0 to minimize the effect of longshore transport and abrasions of the stones. Burcharth and Frigaard (1987) and later van der Meer and Veldman (1992) investigated longshore transport of berm breakwaters; and concluded that to minimize the effect of longshore transport, the stability number must be less than 3. In this way, the measured recessions were mostly within the range mentioned in Table 1. As mentioned earlier, berm breakwaters with higher stability numbers are not considered as statically stable structures. In addition, experiments were conducted with an emerged berm to get the full benefit of the berm in the overall stability. The berm width ranges were chosen to be close to

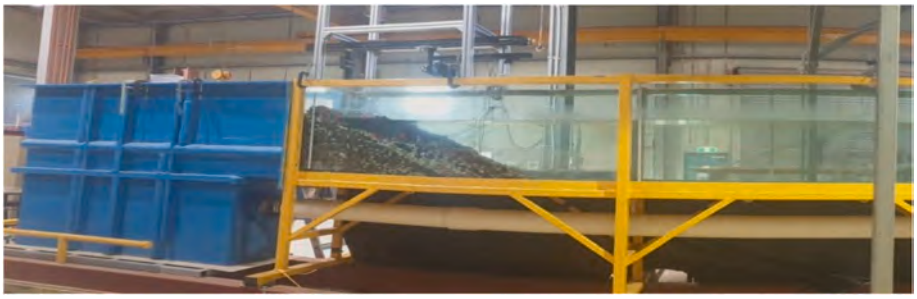

Fig. 3. Longitudinal cross-section of the flume of Griffith University and the constructed model.

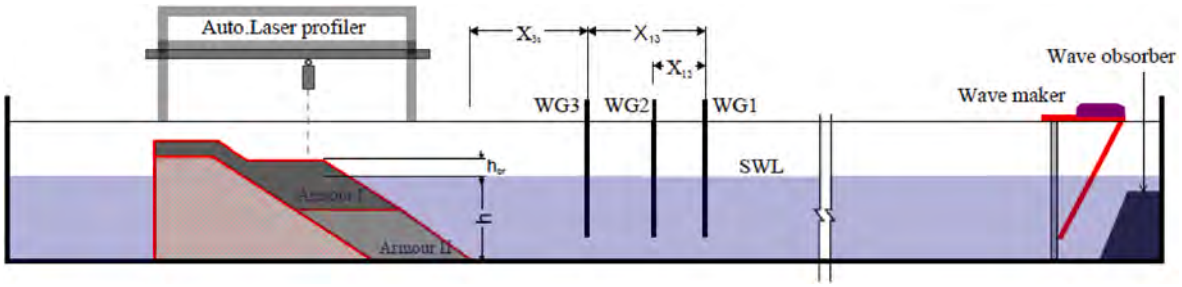

Fig. 4. Sketch of the experimental set-up.

Table 3
Used rock characteristics.

	Armour Layer I	Armour Layer II	Core
W_{50} (kg)	0.035	0.014	0.0039
D_{n50} (mm)	23.2	17	11.5
f_g=D_{n85}/D_{n15}	1.2	1.45	1.4
ρ_s (kg/m^3)	2800	2800	2800

the optimum design. The structural front slope was a non-steep front slope (1:1.5).

A non-contact laser profiler (Fig. 4) consisting of 7 laser pointers was used to measure the initial and reshaped profile. The distance between the laser pointer was 0.045 m and the interval between each measurement point in a profile was 0.02 m (keeping the edge lasers at a safe distance from the flume wall to eliminate the wall effects). An average of 7 profiles was used to report the measurements. The recession and the erosion depth were also obtained from these measurements.

The cumulative method was used to measure the recession of 26 test series. Each test series consists of 4 different wave steps. Wave height increased steadily in each test series and the reshaped profile was measured after each test (1500 waves) and then the structure was rebuilt. For each test series, the initial profile was measured first. Two cameras were installed to monitor the structure during the experiment. One side camera was used to take photos regularly during the tests, and the other was used for video recording of the reshaping of the structure during the tests. Test matrix of experiments is provided in Appendix A.

4. Results and discussion

4.1. Berm recession, Rec

4.1.1. Influence of the stability number

Fig. 5 shows the influence of H_0 on the recession (grouped by dimensionless wave period) and, as expected, the recession increases as the stability number (i.e. the destabilising force) increases and as the wave breaks on the structure more turbulent flow will act on the rocks (Moghim et al., 2011). Additionally, wave run-up increases as the wave height increases and it was observed that the upward force generated by the wave run-up essentially lifts the rocks, potentially causing destabilization by disrupting their arrangement or positioning within the berm structure. This upward movement can make the rocks more susceptible to subsequent run-down action when the waves retreat, leading to the dislodgement and rolling down of already unstable rocks due to the force exerted by the waves.

Fig. 6 represents the reshaped profiles of an example set of sea states (four stability numbers) with the same dimensionless wave period, T_0 = 27, which aligns with the pattern observed in Fig. 5. It shows that by increasing the stability number (i.e., energy), the reshaping of the berm profile becomes more pronounced.

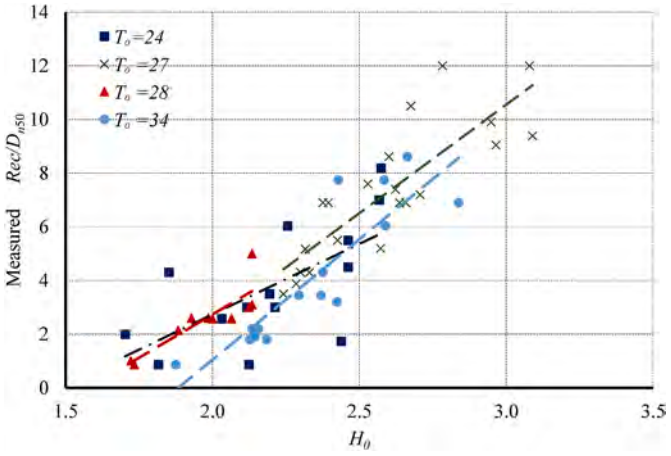

Fig. 5. Influence of the stability number, H_0, on the berm recession (Rec/D_{n50}). The dashed lines represent the linear trend of tests grouped by the dimensionless wave period.

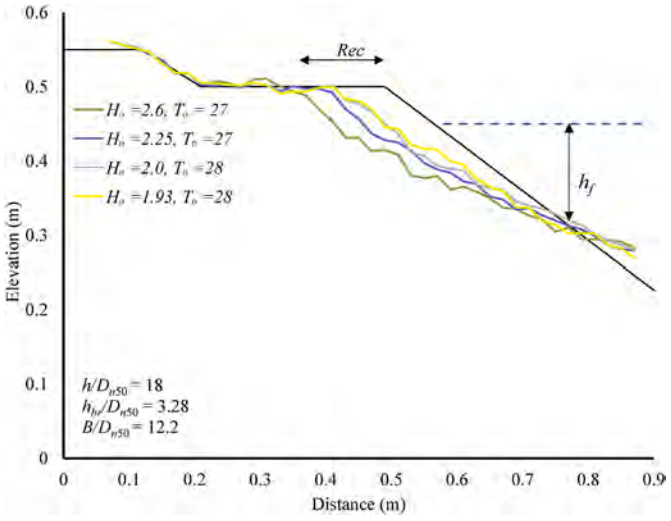

Fig. 6. Typical influence of stability no on the reshaped structure profile.

4.1.2. Influence of the dimensionless wave period

Fig. 7 shows that the effect of the Dimensionless wave period (with constant stability number) on the berm recession is less obvious. In some cases, the recession increases slightly with increasing dimensionless wave period but for some other cases, it is the opposite. Ehsani et al. (2020) found that for the Icelandic-type berm breakwater, the type of wave breaking plays a significant role in the berm recession. To examine this, the Iribarren number is often used to differentiate between the plunging and surging waves, especially for hardly reshaped berm

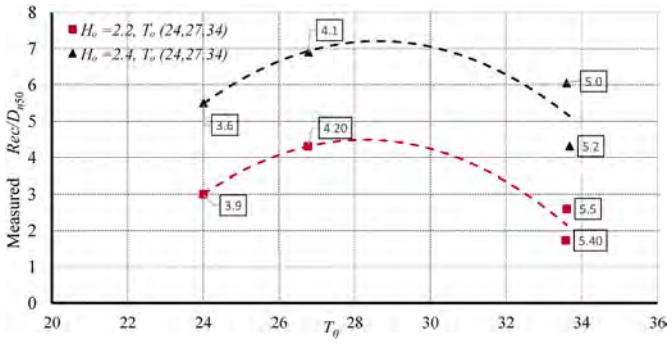

Fig. 7. Influence of dimensionless wave period, T_0, on the berm recession. Numbers in the text box annotations represent the Iribarren numbers. The dashed (second-degree polynomial) lines represent the trend of experimental tests grouped by stability no.

breakwaters and conventional breakwaters (Van der Meer, 1988). The Iribarren number (Ir_{op}) is defined as:

$$Ir_{op} = \tan\alpha / \sqrt{s_{op}} \tag{26}$$

Where tan α is the initial slope of the berm, s_{op} is the wave steepness defined as:

$$s_{op} = H_S / L_{OP} \tag{27}$$

Where L_{op} is the deep water wavelength based on the peak period.

EurOtop (2018) classifies plunging waves as having Iribarren numbers in the range 2–3 for conventional breakwaters, and the transition status between plunging waves and surging waves is known as collapsing. For collapsing waves, the wavefront becomes almost vertical and the water excursion on the slope (wave run-up + run-down) is often larger; and as stated above, the run-down led to the displacement and rolling of the rocks.

Fig. 7 also implies that the berm recession slightly increases as the Iribarren number becomes critical (Iribarren number about 4.2, surging wave type), and when it exceeds this value the berm recession starts reducing. It should be mentioned that this preliminary finding is based on a limited number of tests and more experiments are required to validate it. It was also observed that the type of breaking wave on the berm breakwater determines the amount of damage and the run-up height (and hence the wave overtopping). Ehsani et al. (2020) also reported that by increasing the Iribarren number to about 4.2, the eroded area becomes larger and after that, it reduces.

4.1.3. Effect of the dimensionless berm height, h_{br}/D_{n50}

Fig. 8 illustrates the influence of the dimensionless berm height (h_{br}/D_{n50}) on the berm recession. Three berm heights were examined (h_{br} = 0.03 m, 0.045 m and 0.075m) with the same set of wave heights (H_s = 0.075 m, 0.095 m, 0.11 m, and 0.123 m). Fig. 8 shows that, as the dimensionless berm height increases, the berm recession decreases which is expected because the purpose of a berm is to act as a cushion to absorb the wave energy during wave attack. However, a very high berm may mimic traditional breakwater behaviour and does not allow the wave to reach the berm which means that the berm will not participate in absorbing the wave energy. Lykke Andersen et al. (2012) also reported that the damage might occur locally similar to the conventional breakwaters for a high berm structure with a gentle front slope. Therefore, an optimal balance in berm elevation is crucial for the performance of the berm breakwaters. Our results indicate that the higher the berm, the less the recession; which is in agreement with the previous findings. Lykke Andersen and Burcharth (2010) showed that as the berm height increases, the recession reduces (equation (5)). In addition, Ehsani et al. (2020) stated that a higher berm enhances stability by dissipating more energy and reducing wave run-up and rundown. Earlier Van der Meer and Sigurdarson (2016) suggested that the ideal berm height is $\geq 0.6\ H_{sD}$.

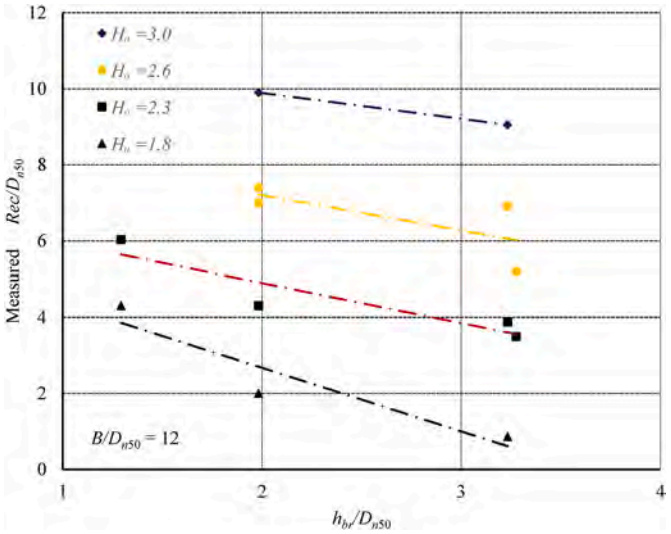

Fig. 8. Influence of berm height h_{br}/D_{n50} on berm recession (Rec/D_{n50}).

4.1.4. Effect of dimensionless berm width (B/D_{n50})

In addition to berm height, berm width plays a role in the design and efficiency of the berm breakwater as a wide berm increases the construction cost dramatically, while a narrow one reduces the geometrical stability. Hence, an optimized berm width is very important in the design of berm breakwater. Fig. 9 illustrates the influence of the berm width (B/D_{n50}) on the berm recession based on tests conducted using two berm widths: 7 D_{n50} and 12 D_{n50} with the narrower berm width (7 D_{n50}) within the design range (Van der Meer and Sigurdarson, 2016). As seen, the berm width in the range of $7.1 < B/D_{n50} < 12.2$ and H_0 = 2.1–2.55 has a negligible effect on the recession. This is in line with previous similar studies. For example, Moghim et al. (2011) also mentioned that berm width has no significant effect on berm recession partly because the tested berms were wide enough to absorb wave energy.

4.1.5. Effect of water depth at the structure toe

Fig. 10 shows that the dimensionless water depth (h/H_s) has a significant impact on the berm recession except for the values of (h/H_s) larger than 5 where the impact becomes less. Different water depths (h = 0.4 m, 0.425 m, 0.45 m, and 0.475 m) were tested with different sets

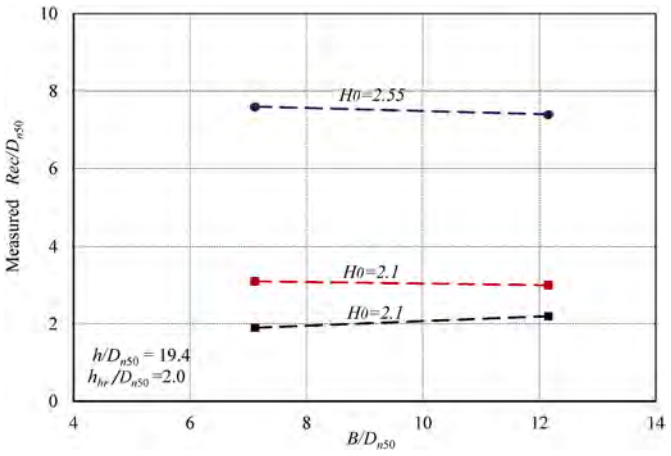

Fig. 9. Influence of dimensionless berm width, B/D_{n50} on berm recession (Rec/D_{n50}).

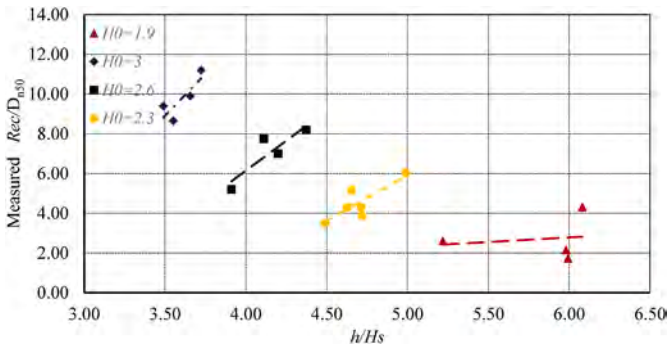

Fig. 10. Influence of water depth, h/H_s on berm recession, Rec/D_{n50}.

of wave heights (H_s = 0.079 m, 0.095 m, 0.11 m, and 0.125 m) and it was found that for the same wave height, as the water depth increases the berm recession increases except for the smallest wave height group ($H_0 = 1.9$). This is because the intersection point between the initial and reshaped profile becomes lower as the water depth increases, leading to more volume of eroded rocks and hence more berm recession. Moghim and Lykke Andersen (2015) also argued that the damage caused by the wave force is proportional to the wave momentum flux which is higher in deeper waters.

Furthermore, it can be seen that for small wave height (low stability number) the influence of the water depth on the recession is much less than that for the large wave height (high stability number) which is in line with Sigurdarson and Van der Meer (2013) scoring system.

4.1.6. *Effect of number of waves*

Generally, when breakwaters are exposed to more waves, the structure will experience more damage up to a limiting equilibrium state. Some researchers such as Moghim and Lykke Andersen (2015) and Shafieefar et al. (2020) include a modification factor to account for the effect of N_w in their formulas in the form of $f(N_w) = N_w^b$, where b varies between 0.07 and 0.3 according to the stability number of the structure. Lykke Andersen and Burcharth (2010) developed an alternative correction factor as a function of the stability number i.e., if the structure is strong $H_0 < 5.0$ the correction factor will be higher while for dynamically reshaped berm breakwater $H_0 > 5.0$ the effect is less. This is because for fully reshaped berm breakwaters most of the deformations would happen earlier at the first 1000 waves. Moghim et al. (2011) and Shekari and Shafieefar (2013) gave more weight to the modification factor than Lykke Andersen and Burcharth (2010) and in both formulas they indicated that more than 90 % of the final recession occurred before $N_w = 3000$ and consequently adopted $N_w = 3000$ for their experiments.

Akbari et al. (2022) found that for the statically stable structure ($40 < H_0T_0 < 80$), the modification factor increases as H_0T_0 increases, while for the dynamically stable structures, this factor decreases as H_0T_0 increases, in line with Lykke Andersen and Burcharth (2010) study.

Fig. 11 shows that in the present experiments, approximately 90% of the final recession occurred in the first 3000 waves, and at $N_w = 1000$ about 80% of the final recession took place in the fully reshaped berm breakwater. While at $N_w = 1000$, about 70% of the final recession happened in the partially reshaped berm breakwater. This is because as the stability number increases, the effects of early sea state increases, which is in line with Moghim et al. (2011) conclusion that the maximum development of the reshaped profile occurs in the first phase of wave attack (a few hundred waves), and 90% of the total reshaping happens before $N_w = 3000$. Shafieefar et al. (2020) examined the influence of storm duration for the berm breakwater and found that 90% of the final reshaped profile occurred before 1500 waves. Our limited tests also shows the same and indicate that Lykke Andersen and Burcharth (2010) formula performs best in predicting the influence of number of waves.

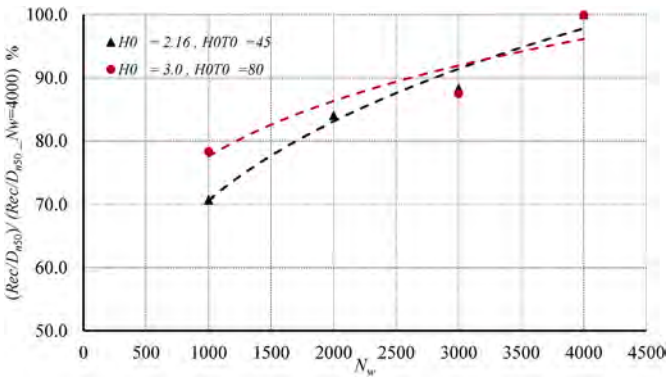

Fig. 11. Influence of number of waves, N_w, on normalized berm recession; different stability numbers.

4.2. *Evaluation of the existing recession formulae*

The scatter diagrams of the estimated and the measured dimensionless recession (Rec/D_{n50}) values for each tested formula are shown in Fig. 12 for the different recession formulas.

Fig. 12a shows that Tørum, (2007) formula overestimated the recession for lower recession values, while underestimation is clear for large recession values. This discrepancy across the range might indicate limitations in its applicability. Figs. 12c and d show that the Moghim et al. (2011) and Shekari and Shafieefar (2013) formulas overestimate the recession. This could be because their formula was developed for steep berm breakwaters with a slope of 1:1.25. As discussed by Sigurdarson and Van der Meer (2013), berm breakwaters with slopes steeper than 1:1.5 will experience more recession, which might contribute to the overestimation seen in these formulas. On the contrary, Fig. 12b shows

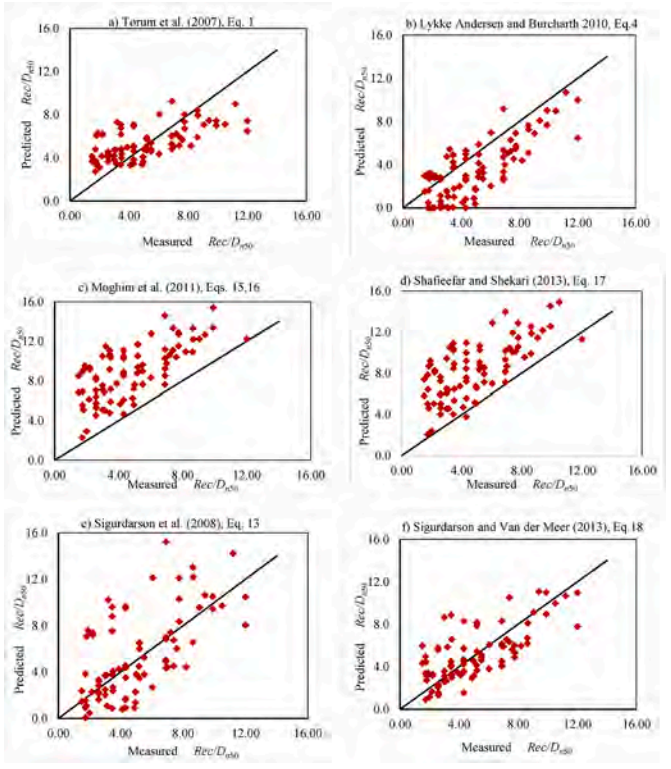

Fig. 12. Comparison between the Measured Rec/D_{n50} and the Predicted one using different formulas. a) Tørum et al., (2003), b) Lykke Andersen, (2006), c) Moghim et al., (2011), d) Shekari and Shafieefar, (2013), e) Sigurdarson et al., (2008) and f) Sigurdarson and Van der Meer, (2013).

that Lykke Andersen and Burcharth, (2010) formula underestimates measured berm recessions, probably because their tests were conducted in a shallower relative depth (h/H_s), which might have influenced the estimated recession.

Figs. 12e and f show that Sigurdarson et al. (2008) and Sigurdarson and Van der Meer (2013) formulas perform better in predicting the recession. Nevertheless, the uncertainty in the prediction is greater when using Sigurdarson et al. (2008) formula, possibly because it considers the influence of the wave period in its form. Van der Meer and Sigurdarson (2016) also found that by using the term (T_0H_0), the scatter will increase.

The performance of the existing models was also quantitatively compared using accuracy metrics such as Normalized Bias (*NBIAS*), Mean Square Error (*MSE*), the scatter index (*SI*), and Discrepancy Ratio (*DR*); defined as follows:

$$NBIAS = \frac{\frac{1}{N}\sum_{i=1}^{N}(P_i - O_i)}{\frac{1}{N}\sum_{i=1}^{N}O_i} \times 100 \tag{28}$$

where N is the number of measurements, P_i is the predicted value, and O_i is the measured one.

$$MSE = \frac{1}{N}\sum_{i=1}^{N}(P_i - O_i)^2 \tag{29}$$

$$SI = \frac{\sqrt{\frac{1}{N}\sum_{i=1}^{N}(P_i - O_i)^2}}{\frac{1}{N}\sum_{i=1}^{N}O_i} \times 100 \tag{30}$$

$$DR_i = \frac{P_i}{O_i} \tag{31}$$

The accuracy metrics of different models are given in Table 4.

It can be seen from Table 4 that most of the accuracy metrics of the Sigurdarson and Van der Meer (2013) formula are better than those of other models, even though it slightly overestimates the recession in this case. This implies that this formula can be used safely for the design of two-layer armour berm breakwaters.

4.3. Erosion depth, h_f

Fig. 13 indicates the relation between the dimensionless erosion depth (h_f/D_{n50}) and the dimensionless water depth (h/D_{n50}). As shown, formulas of Tørum et al. (2003) and Moghim and Lykke Andersen (2015) provide a very conservative estimation of the erosion depth in this case.

This figure also suggests uncertainty when using water depth (h/D_{n50}) to predict the erosion depth (h_f/D_{n50}). To address this issue, a new formula is proposed to predict the erosion depth as a function of the dimensionless depth parameter (h/H_s). The following formula aims to establish a better relationship between the erosion depth and the ratio of water depth to wave height, suggesting that this parameter might offer a more accurate prediction of erosion depth:

$$\frac{h_f}{H_s} = 0.2\frac{h}{H_s} + 0.25 \tag{32}$$

Table 4
Accuracy metrics of different formulae for (all) tests.

Formula	*NBIAS*%	*MSE*	*SI* %	*DR*
Tørum et al. (2003)	8.1	4.5	43.1	1.30
Lykke Andersen (2006)	−28.5	5.0	45.4	0.69
Sigurdarson et al. (2008)	8.1	7.9	57.1	1.18
Sigurdarson and Van der Meer (2013)	2.4	3.9	40.1	1.20

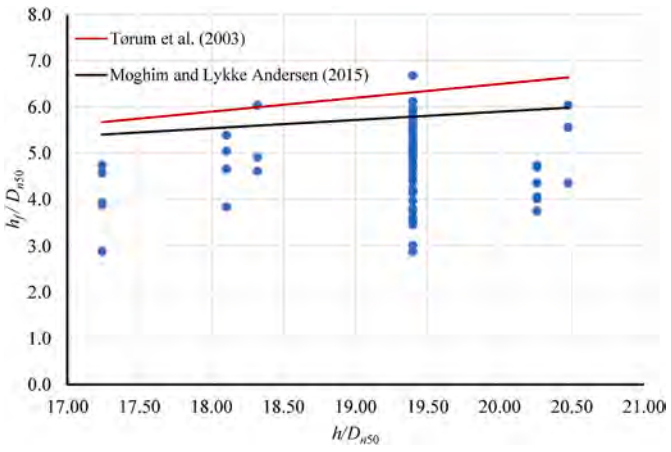

Fig. 13. Evaluation of Tørum et al. (2003) and Moghim and Lykke Andersen (2015) equations using present experimental data.

Equation (32) is valid with a standard deviation of 10 % for $1.2 < H_0 < 3.1$, $3.5 < \frac{h}{H_s} < 9.4$, $17.2 < \frac{h}{D_{n50}} < 20.5$ and $7.1 < \frac{B}{D_{n50}} < 12.2$.

Fig. 14 demonstrates that Eq. (32), i.e., the relationship between erosion depth normalized by wave height (h_f/H_s) and the ratio of water depth to wave height (h/H_s) performs better compared to the previous formulas. Fig. 14 shows that as the water depth increases, there is a corresponding increase in erosion depth.

This formula indicates that as the water depth increases (and more volume of rocks needs to be moved before reaching a stable profile), the depth of erosion increases to balance the eroded volume. This clarity in the relationship could potentially enhance the predictive accuracy of erosion depth. Furthermore, it was found that the erosion depth h_f range is about (3.5–4) D_{n50} of the top layer. This was echoed in the previous studies (e.g. Tørum et al., 2003) and leads to the following for the thickness of top layer in two-class armour berm breakwaters:

$$\text{Thickness of Top layer} \geq 4\, D_{n50} \quad \text{Class I} \tag{33}$$

This suggested thickness of the top layer is almost double of the value suggested by Sveinbjörnsson (2008), which was derived for Icelandic-type berm breakwaters. The reason for that is probably the narrower grading in class I in Icelandic-type compared to that of the two-class armour berm breakwater being examined in this study. The variation in rock sizes and the arrangement within different classes or types of berm breakwaters can lead to significant differences in erosion depth and subsequently affect the thickness required for different classes or layers within these structures. Considering this fact is crucial for accurate design and performance requirements.

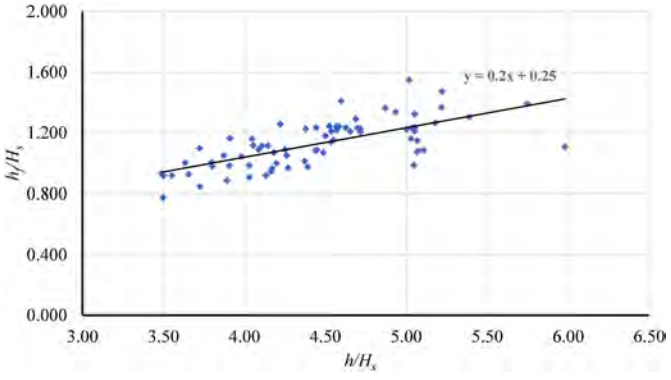

Fig. 14. Influence of relative water depth, h/H_s, on the erosion depth (h_f/H_s).

5. Conclusions

Effects of sea state conditions and the geometrical parameters on the stability of the two-class armour berm breakwaters were investigated by conducting a series of 110 tests in a small scale wave flume. Tests covered a wide range of wave parameters and geometrical conditions. This study aimed to provide a new design criterion for the stability of the two-class armour berm breakwaters. It should be mentioned that the focus of this study was on partly reshaped berm breakwaters, which are more common. Hence from a total of 110 experiments, 85 tests were conducted on the PR berm breakwaters and 25 tests on the HR ones. The following conclusions can be utilized from the present study:

- It is advantageous to split the wide-graded armour layer of mass armour berm breakwaters into two layers with narrower grading and laying larger rocks on the top. This will increase the stability, in line with the findings of Juhl and Sloth (1998), with minimum extra cost for grading.
- The comparison of formulas derived specifically for mass armour and Icelandic-type berm breakwaters showed that Sigurdarson and Van der Meer (2013) equation yields a better (and somehow conservative) estimation for the recession of two-class armour berm breakwaters. Therefore, this formula can be used to estimate the berm recession by using D_{n50} of the armour layer I in the formula.
- The berm height above SWL plays a considerable role in increasing the stability of the two-class armour berm breakwaters. An optimal berm elevation is important for the performance of the berm breakwaters, dissipating more wave energy and reducing the effect of wave run-up and run-down on destabilizations of the berm rocks.
- The berm width within the tested ranges of $7.1 < B/D_{n50} < 12.2$ and $2.1 < H_0 < 2.55$ had an insignificant effect on the recession. Hence, a very wide berm may not increase the stability necessarily in PR berm breakwaters.
- A new formula was introduced for the prediction of erosion depth as a function of the dimensionless depth parameter (h/Hs). The new formula performs better than the other existing formulas.

CRediT authorship contribution statement

Mohammed Al-Ogaili: Writing – original draft, Validation, Methodology, Investigation, Formal analysis, Data curation, Conceptualization. **Amir Etemad-Shahidi:** Writing – review & editing, Supervision, Methodology, Formal analysis, Conceptualization. **Nick Cartwright:** Writing – review & editing, Supervision, Software, Conceptualization. **Sigurdur Sigurdarson:** Writing – review & editing, Supervision, Conceptualization.

Declaration of competing interest

The authors declare that they have no known competing financial interests or personal relationships that could have appeared to influence the work reported in this paper.

Data availability

Data will be made available on request.

Acknowledgement

The staff of the Hydraulic laboratory at Griffith University are acknowledged for their support.

Appendix. A

Table A-1
Summary of the formulas input parameters and type of structures used in experiments.

Parameters	Formulae					
	Tørum et al. (2003/2007)	Lykke Andersen (2006)	Sigurdarson et al. (2008)	Moghim et al. (2011)	Shekari and Shafieefar (2013	Sigurdarson and Van der Meer (2013)
H_0		X				X
H_0T_0	X		X			
$H_0\sqrt{T_0}$				X	X	
s_{0m}		X				
f_g	X	X				
h	X	X		X		
Nw		X		X	X	
β		X				
h_{br}		X		X	X	
B					X	
$Skewness$		X				
$cot(\alpha)$		X				
Type	MA/IC	MA	IC	MA	MA	MA/IC

Note * = In Sigurdarson and Van der Meer (2013) the influence of h/H_s, h_{br}/H_s and $cot(\alpha)$ are considered separately as a scoring system.

Table A-2
Summary of the formulas' limitations.

Parameters	Formulae					
	Tørum et al. (2003-7)	Lykke Andersen (2006)	Sigurdarson et al. (2008)	Moghim et al. (2011)	Shekari and Shafieefar (2013)	Sigurdarson and Van der Meer (2013)
H_0		0.96–4.86				<3.0
H_0T_0	> 20-30	16.8–163	<70			
$H_0\sqrt{T_0}$				7.7–24.4	7.09–23.5	

(*continued on next page*)

Table A-2 (*continued*)

Parameters	Formulae					
	Tørum et al. (2003-7)	Lykke Andersen (2006)	Sigurdarson et al. (2008)	Moghim et al. (2011)	Shekari and Shafieefar (2013)	Sigurdarson and Van der Meer (2013)
s_{0p}		0.01–0.054				
f_g	1.3 – 1.8			1.2 – 1.5		
h/D_{n50}	12.5 – 25	8.7–22.3		8–16.5	9.6–14.11	
Nw				500–6000	500–6000	
h_{br}/H_s				0.12–1.24	0.22–1.57	
h_{br}/H_{m0}		−0.6–1.79				
B/D_{n50}		7.7 – 33			14 – 29.41	
cot α		1.25		1.25	1.25	

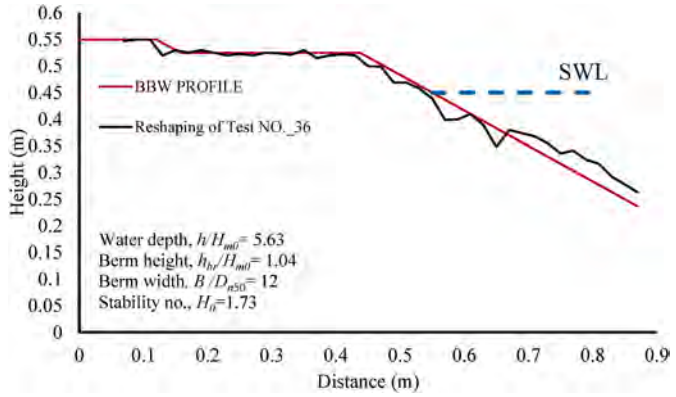

Fig. A-1. The recession profile of a test with a high berm. The type of damage is similar that of conventional breakwaters with minimal recession and damage is mostly on the slope.

A-3 Ehsani et al. (2020) formula

Ehsani et al. (2020) studied the influence of sea states and structural parameters on the stability of Multi-Layer Berm Breakwaters (MLBBs). They found that a wider berm results in lower damage parameters and increasing the height of stone class I improves the stability and reduces damage, up to a certain limit where further increase only adds cost without benefiting stability. It should be noted that the largest stones should extend to the erosion depth. Higher berm elevation from Still Water Level (SWL) enhances stability by dissipating more energy and reducing wave run-up and rundown. Ehsani et al. (2020) mentioned that very high berms increase the damage and reduce the stability. They introduced a new formula set to predict the damage parameter using a new stability parameter, N_{sn}, to estimate the damage parameter as follows:

$$S_d = 3.59\times10^{-4}N_{sn}^{4.52}(\tan\alpha)^{2.64}\left(\frac{B}{D_{n50I}}\right)^{-1}\left(\frac{h_{br}}{D_{n50I}}\right)^{0.5}\left(\frac{h}{D_{n50I}}\right)^{2}$$
$$\left[0.025+exp\left(\left(-0.557\,H_0\sqrt{T_0}+2.97\right)\left(\frac{h_I}{H_s}\right)\right)\right] \quad for\ (Ir_{op}) \le 4.2\ (Plunging\ waves) \tag{A.1}$$

$$S_d = 1.63\times10^{-6}N_{sn}^{6.94}(\tan\alpha)^{2.64}\left(\frac{B}{D_{n50I}}\right)^{-1}\left(\frac{h_{br}}{D_{n50I}}\right)^{0.5}\left(\frac{h}{D_{n50I}}\right)^{2}$$
$$\left[0.025+\exp\left(\left(-0.557\,H_0\sqrt{T_0}+2.97\right)\left(\frac{h_I}{H_s}\right)\right)\right] \quad \text{for } (Ir_{op}) > 4.2\ (\text{Surging waves}) \tag{A.2}$$

where D_{n50I} is the median nominal diameter of the top armour rock, N_{sn} is the stability dimensionless parameter which depends on $H_0\sqrt{T_0}$, h_I is the thickness of top armour layer I, tan α is the initial front slope of the structure and Ir_{op} is the Iribarren number $= \tan\alpha/\sqrt{s_{op}}$.

Table A-3
Accuracy metrics of different formulae including Ehsani et al. (2020).

Formula	*NBIAS%*	*MSE*	*SI %*	*DR*
Tørum et al. (2003)	8.1	4.5	43.1	1.30
Lykke Andersen (2006)	−28.5	5.0	45.4	0.69
Sigurdarson et al. (2008)	8.1	7.9	57.1	1.18
Sigurdarson and Van der Meer (2013)	2.4	3.9	40.1	1.20
Ehsani et al. (2020)	30	25	103	1.4

It should be noted that Ehsani et al. (2020) formula set has been developed to estimate the damage ratio rather than *Rec*. More importantly, the formula has been validated for HR berm breakwater with $1.3 < Ho < 2.6$ while most of our tests were conducted on PR ones with *Ho* up to 3.1.

Table A-4
Test Matrix

Test No	Hs m	Tp s	$T_{(0,1)}$ s	cot α	Nw	Rc m	B m	h_{br} m	Gc m	h m	h_I m	Dn_{50} layer I m	T_0	H_0 layer I
1	0.06	1.2	1.0	1.5	1500	0.100	0.165	0.046	0.12	0.450	0.146	0.0232	20.4	1.4
2	0.07	1.2	1.0	1.5	1500	0.100	0.165	0.046	0.12	0.450	0.146	0.0232	20.4	1.6
3	0.08	1.2	1.0	1.5	1500	0.100	0.165	0.046	0.12	0.450	0.146	0.0232	20.4	2.0
4	0.10	1.2	1.0	1.5	1500	0.100	0.165	0.046	0.12	0.450	0.146	0.0232	20.4	2.3
5	0.09	1.2	1.0	1.5	1500	0.100	0.165	0.046	0.12	0.450	0.146	0.0232	20.4	2.2
6	0.10	1.2	1.0	1.5	1500	0.100	0.165	0.046	0.12	0.450	0.146	0.0232	20.4	2.4
7	0.11	1.2	1.0	1.5	1500	0.100	0.165	0.046	0.12	0.450	0.146	0.0232	20.4	2.5
8	0.12	1.2	1.0	1.5	1500	0.100	0.165	0.046	0.12	0.450	0.146	0.0232	20.4	2.9
9	0.05	1.6	1.3	1.5	1500	0.100	0.165	0.046	0.12	0.450	0.146	0.0232	27.4	1.3
10	0.07	1.6	1.3	1.5	1500	0.100	0.165	0.046	0.12	0.450	0.146	0.0232	27.4	1.6
11	0.08	1.6	1.3	1.5	1500	0.100	0.165	0.046	0.12	0.450	0.146	0.0232	27.4	2.0
12	0.10	1.6	1.3	1.5	1500	0.100	0.165	0.046	0.12	0.450	0.146	0.0232	26.7	2.3
13	0.10	1.6	1.3	1.5	1500	0.100	0.165	0.046	0.12	0.450	0.146	0.0232	26.8	2.3
14	0.11	1.6	1.3	1.5	1500	0.100	0.165	0.046	0.12	0.450	0.146	0.0232	26.8	2.5
15	0.12	1.6	1.3	1.5	1500	0.100	0.165	0.046	0.12	0.450	0.146	0.0232	27.4	2.9
16	0.06	2.0	1.6	1.5	1500	0.100	0.165	0.046	0.12	0.450	0.146	0.0232	33.4	1.5
17	0.08	2.0	1.6	1.5	1500	0.100	0.165	0.046	0.12	0.450	0.146	0.0232	33.5	1.9
18	0.09	2.0	1.6	1.5	1500	0.100	0.165	0.046	0.12	0.450	0.146	0.0232	33.6	2.2
19	0.10	2.0	1.6	1.5	1500	0.100	0.165	0.046	0.12	0.450	0.146	0.0232	33.7	2.3
20	0.09	2.0	1.6	1.5	1500	0.100	0.165	0.046	0.12	0.450	0.146	0.0232	33.6	2.1
21	0.09	2.0	1.6	1.5	1500	0.100	0.165	0.046	0.12	0.450	0.146	0.0232	33.6	2.1
22	0.10	2.0	1.6	1.5	1500	0.100	0.165	0.046	0.12	0.450	0.146	0.0232	33.7	2.4
23	0.10	2.0	1.6	1.5	1500	0.100	0.165	0.046	0.12	0.450	0.146	0.0232	33.7	2.4
24	0.11	2.0	1.6	1.5	1500	0.100	0.165	0.046	0.12	0.450	0.146	0.0232	33.8	2.6
25	0.11	2.0	1.6	1.5	1500	0.100	0.165	0.046	0.12	0.450	0.146	0.0232	33.8	2.6
26	0.05	1.2	1.0	1.5	1500	0.100	0.165	0.075	0.12	0.450	0.175	0.0232	20.2	1.1
27	0.08	1.2	1.0	1.5	1500	0.100	0.165	0.075	0.12	0.450	0.175	0.0232	20.3	1.8
28	0.09	1.2	1.0	1.5	1500	0.100	0.165	0.075	0.12	0.450	0.175	0.0232	21.3	2.1
29	0.09	1.2	1.0	1.5	1500	0.100	0.165	0.075	0.12	0.450	0.175	0.0232	21.3	2.1
30	0.10	1.2	1.0	1.5	1500	0.100	0.165	0.075	0.12	0.450	0.175	0.0232	21.3	2.3
31	0.10	1.2	1.0	1.5	1500	0.100	0.165	0.075	0.12	0.450	0.175	0.0232	21.3	2.5
32	0.09	1.2	1.0	1.5	1500	0.100	0.165	0.075	0.12	0.450	0.175	0.0232	21.3	2.2
33	0.09	1.6	1.3	1.5	1500	0.100	0.165	0.075	0.12	0.450	0.175	0.0232	27.6	2.1
34	0.10	1.6	1.3	1.5	1500	0.100	0.165	0.075	0.12	0.450	0.175	0.0232	26.8	2.4
35	0.11	1.6	1.3	1.5	1500	0.100	0.165	0.075	0.12	0.450	0.175	0.0232	26.9	2.7
36	0.07	1.6	1.3	1.5	1500	0.100	0.282	0.075	0.12	0.450	0.175	0.0232	27.7	1.7
37	0.10	1.6	1.3	1.5	1500	0.100	0.282	0.075	0.12	0.450	0.175	0.0232	26.8	2.3
38	0.11	1.6	1.3	1.5	1500	0.100	0.282	0.075	0.12	0.450	0.175	0.0232	26.8	2.7
39	0.12	1.6	1.3	1.5	1500	0.100	0.282	0.075	0.12	0.450	0.175	0.0232	26.9	3.0
40	0.09	1.6	1.3	1.5	1500	0.100	0.282	0.046	0.12	0.450	0.146	0.0232	27.6	2.1
41	0.10	1.6	1.3	1.5	1500	0.100	0.282	0.046	0.12	0.450	0.146	0.0232	26.8	2.3
42	0.11	1.6	1.3	1.5	1500	0.100	0.282	0.046	0.12	0.450	0.146	0.0232	26.8	2.6
43	0.12	1.6	1.3	1.5	1500	0.100	0.282	0.046	0.12	0.450	0.146	0.0232	26.9	2.9
44	0.06	1.4	1.2	1.5	1500	0.150	0.282	0.100	0.12	0.400	0.200	0.0232	23.9	1.5
45	0.08	1.4	1.2	1.5	1500	0.150	0.282	0.100	0.12	0.400	0.200	0.0232	24.0	2.0
46	0.09	1.4	1.2	1.5	1500	0.150	0.282	0.100	0.12	0.400	0.200	0.0232	24.0	2.1
47	0.08	1.6	1.3	1.5	1500	0.080	0.282	0.030	0.12	0.470	0.130	0.0232	27.7	1.9
48	0.08	1.4	1.2	1.5	1500	0.080	0.282	0.030	0.12	0.470	0.130	0.0232	24.0	1.9
49	0.09	1.4	1.2	1.5	1500	0.080	0.282	0.030	0.12	0.470	0.130	0.0232	24.0	2.3
50	0.11	1.4	1.2	1.5	1500	0.080	0.282	0.030	0.12	0.470	0.130	0.0232	24.0	2.6
51	0.06	1.4	1.2	1.5	1500	0.100	0.282	0.046	0.12	0.450	0.146	0.0232	24.1	1.5
52	0.07	1.4	1.2	1.5	1500	0.100	0.282	0.046	0.12	0.450	0.146	0.0232	24.1	1.7
53	0.09	1.4	1.2	1.5	1500	0.100	0.282	0.046	0.12	0.450	0.146	0.0232	24.0	2.2
54	0.10	1.4	1.2	1.5	1500	0.100	0.282	0.046	0.12	0.450	0.146	0.0232	24.0	2.5
55	0.11	1.4	1.2	1.5	1500	0.100	0.282	0.046	0.12	0.450	0.146	0.0232	24.0	2.6
56	0.07	1.4	1.2	1.5	1500	0.150	0.282	0.075	0.12	0.400	0.121	0.0232	24.0	1.6
57	0.09	1.4	1.2	1.5	1500	0.150	0.282	0.075	0.12	0.400	0.121	0.0232	24.0	2.2
58	0.10	1.4	1.2	1.5	1500	0.150	0.282	0.075	0.12	0.400	0.121	0.0232	24.0	2.5
59	0.10	1.5	1.3	1.5	1500	0.150	0.282	0.075	0.12	0.400	0.121	0.0232	25.8	2.4
60	0.07	1.2	1.0	1.5	1500	0.100	0.282	0.046	0.12	0.450	0.146	0.0232	20.4	1.6
61	0.09	1.2	1.0	1.5	1500	0.100	0.282	0.046	0.12	0.450	0.146	0.0232	20.4	2.1
62	0.10	1.2	1.0	1.5	1500	0.100	0.282	0.046	0.12	0.450	0.146	0.0232	20.4	2.3
63	0.11	1.2	1.0	1.5	1500	0.100	0.282	0.046	0.12	0.450	0.146	0.0232	20.4	2.6
64	0.12	1.2	1.0	1.5	1500	0.100	0.282	0.046	0.12	0.450	0.146	0.0232	20.4	2.9
65	0.08	2.0	1.6	1.5	1500	0.100	0.282	0.046	0.12	0.450	0.146	0.0232	33.7	1.9
66	0.09	2.0	1.6	1.5	1500	0.100	0.282	0.046	0.12	0.450	0.146	0.0232	33.7	2.2
67	0.10	2.0	1.6	1.5	1500	0.100	0.282	0.046	0.12	0.450	0.146	0.0232	33.7	2.4
68	0.12	2.0	1.6	1.5	1500	0.100	0.282	0.046	0.12	0.450	0.146	0.0232	33.8	2.8
69	0.07	1.6	1.3	1.5	1500	0.100	0.282	0.046	0.12	0.450	0.146	0.0232	27.7	1.7
70	0.09	1.6	1.3	1.5	1500	0.100	0.282	0.046	0.12	0.450	0.146	0.0232	27.7	2.1
71	0.10	1.6	1.3	1.5	1500	0.100	0.282	0.046	0.12	0.450	0.146	0.0232	26.8	2.4
72	0.11	1.6	1.3	1.5	1500	0.100	0.282	0.046	0.12	0.450	0.146	0.0232	26.9	2.6
73	0.08	1.7	1.4	1.5	1500	0.130	0.282	0.076	0.12	0.420	0.146	0.0232	28.4	1.9
74	0.08	1.7	1.4	1.5	1500	0.130	0.282	0.076	0.12	0.420	0.146	0.0232	28.5	2.0
75	0.09	1.6	1.3	1.5	1500	0.130	0.282	0.076	0.12	0.420	0.146	0.0232	26.9	2.2

(*continued on next page*)

Table A-4 (*continued*)

Test No	*Hs* m	*Tp* s	$T_{(0,1)}$ s	cot α	*Nw*	*Rc* m	*B* m	h_{br} m	*Gc* m	*h* m	*hɪ* m	Dn_{50} layer ɪ m	T_0	H_0 layer ɪ
76	0.11	1.6	1.3	1.5	1500	0.130	0.282	0.076	0.12	0.420	0.146	0.0232	27.0	2.6
77	0.09	1.2	1.0	1.5	1500	0.200	0.282	0.046	0.12	0.450	0.146	0.0232	20.4	2.1
78	0.10	1.2	1.0	1.5	1500	0.200	0.282	0.046	0.12	0.450	0.146	0.0232	20.4	2.4
79	0.11	1.2	1.0	1.5	1500	0.200	0.282	0.046	0.12	0.450	0.146	0.0232	20.4	2.6
80	0.12	1.2	1.0	1.5	1500	0.200	0.282	0.046	0.12	0.450	0.146	0.0232	20.4	2.8
81	0.09	2.0	1.6	1.5	1500	0.200	0.282	0.046	0.12	0.450	0.146	0.0232	33.7	2.1
82	0.10	2.0	1.6	1.5	1500	0.200	0.282	0.046	0.12	0.450	0.146	0.0232	33.8	2.4
83	0.11	2.0	1.6	1.5	1500	0.200	0.282	0.046	0.12	0.450	0.146	0.0232	33.8	2.7
84	0.09	1.6	1.3	1.5	1500	0.150	0.282	0.046	0.12	0.450	0.146	0.0232	27.7	2.1
85	0.10	1.6	1.3	1.5	1500	0.150	0.282	0.046	0.12	0.450	0.146	0.0232	26.8	2.4
86	0.11	1.6	1.3	1.5	1500	0.150	0.282	0.046	0.12	0.450	0.146	0.0232	26.9	2.6
87	0.12	1.6	1.3	1.5	1500	0.150	0.282	0.046	0.12	0.450	0.146	0.0232	26.9	2.8
88	0.09	1.2	1.0	1.5	1000	0.150	0.282	0.046	0.12	0.450	0.146	0.0232	20.4	2.2
89	0.09	1.2	1.0	1.5	2000	0.150	0.282	0.046	0.12	0.450	0.146	0.0232	20.3	2.1
90	0.10	1.2	1.0	1.5	3000	0.150	0.282	0.046	0.12	0.450	0.146	0.0232	20.6	2.4
91	0.09	1.2	1.0	1.5	4000	0.150	0.282	0.046	0.12	0.450	0.146	0.0232	21.3	2.1
92	0.13	1.6	1.3	1.5	1000	0.150	0.282	0.046	0.12	0.450	0.146	0.0232	26.9	3.1
93	0.13	1.6	1.3	1.5	2000	0.150	0.282	0.046	0.12	0.450	0.146	0.0232	26.8	3.1
94	0.13	1.6	1.3	1.5	3000	0.150	0.282	0.046	0.12	0.450	0.146	0.0232	26.8	3.0
95	0.13	1.6	1.3	1.5	4000	0.150	0.282	0.046	0.12	0.450	0.146	0.0232	26.8	3.1
96	0.08	1.4	1.2	1.5	1500	0.130	0.282	0.046	0.12	0.450	0.146	0.0232	24.3	1.8
97	0.09	1.4	1.2	1.5	1500	0.130	0.282	0.046	0.12	0.450	0.146	0.0232	24.3	2.1
98	0.10	1.4	1.2	1.5	1500	0.130	0.282	0.046	0.12	0.450	0.146	0.0232	24.3	2.4
99	0.12	1.5	1.2	1.5	1500	0.130	0.282	0.046	0.12	0.450	0.146	0.0232	24.9	2.8
100	0.07	1.0	0.9	1.5	1500	0.090	0.282	0.026	0.12	0.470	0.146	0.0232	17.6	1.6
101	0.11	1.2	1.0	1.5	1500	0.090	0.282	0.026	0.12	0.470	0.146	0.0232	20.5	2.6
102	0.12	1.2	1.0	1.5	1500	0.090	0.282	0.026	0.12	0.470	0.146	0.0232	20.5	2.8
103	0.13	1.2	1.0	1.5	1500	0.090	0.282	0.026	0.12	0.470	0.146	0.0232	20.4	3.0
104	0.09	1.8	1.5	1.5	1500	0.135	0.282	0.076	0.12	0.425	0.146	0.0232	30.5	2.1
105	0.10	1.8	1.5	1.5	1500	0.135	0.282	0.076	0.12	0.425	0.146	0.0232	30.5	2.4
106	0.11	1.8	1.5	1.5	1500	0.135	0.282	0.076	0.12	0.425	0.146	0.0232	30.5	2.6
107	0.12	1.8	1.5	1.5	1500	0.135	0.282	0.076	0.12	0.425	0.146	0.0232	30.5	2.9
108	0.09	1.8	1.5	1.5	1500	0.085	0.282	0.026	0.12	0.475	0.146	0.0232	30.4	2.2
109	0.10	1.8	1.5	1.5	1500	0.085	0.282	0.026	0.12	0.475	0.146	0.0232	30.5	2.5
110	0.13	1.8	1.5	1.5	1500	0.125	0.282	0.026	0.12	0.475	0.146	0.0232	30.5	3.1

References

Akbari, H., Karami Matin, A.A., Shafieefar, M., 2022. The effect of sequential storms on the performance of homogeneous berm breakwaters. Coast Eng. 175, 104141 https://doi.org/10.1016/j.coastaleng.2022.104141.

Al-Ogaili, M., Etemad-Shahidi, A., Cartwright, N., Sigurdarson, S., 2022. The stability of berm breakwaters, state of art and sensitivity analysis. Coast Eng. 172, 104059 https://doi.org/10.1016/j.coastaleng.2021.104059.

Burcharth, H.F., Frigaard, P., 1987. Reshaping Breakwaters: on the stability of roundheads and trunk erosion in oblique waves. In: Proceedings of the Berm Type Breakwater Conference. Canada. September 1987.

Ehsani, M., Moghim, M.N., Shafieefar, M., 2020. An experimental study on the hydraulic stability of Icelandic-Type berm breakwaters. Coast Eng. 156 https://doi.org/10.1016/j.coastaleng.2019.103599.

EurOtop, 2018. Stability of rubble mound breakwaters—a study of the notional permeability factor, based on physical model tests. Water 11, 934.

Juhl, J., Sloth, P., 1998. Berm breakwaters - influence of stone gradation, permeability and armouring. Proc. Coast. Eng. Conf. 2, 1394–1406. https://www.scopus.com/inward/record.uri?eid=2-s2.0-0032257392&partnerID=40&md5=57a77544f8837134a495a185f1075171.

Klopman, G., Van Der Meer, J.W., 1999. Random wave measurements in front of reflective structures. J. Waterw. Port, Coast. Ocean Eng. 125 (1), 39–45. https://doi.org/10.1061/(ASCE)0733-950X(1999)125:139.

Lykke Andersen, T., 2006. Hydraulic Response of Rubble Mound Breakwaters. Scale Effects-Berm Breakwaters. Department of Civil Engineering, Aalborg University, Denmark. PhD Thesis.

Lykke Andersen, T., Burcharth, H.F., 2010. A new formula for front slope recession of berm breakwaters. Coast Eng. 57 (4), 359–374. https://doi.org/10.1016/j.coastaleng.2009.10.017.

Lykke Andersen, T., Van Der Meer, J.W., Burcharth, H.F., Sigurdarson, S., 2012. Stability of hardly reshaping berm breakwaters. In: Proceedings of the Coastal Engineering Conference. https://doi.org/10.9753/icce.v33.structures.17.

Mansard, E.P., Funke, E., 1980. The measurement of incident and reflected spectra using a least squares method. Coast Eng. 1980, 154–172.

Moghim, M.N., Lykke Andersen, T., 2015. Armor stability of hardly (or partly) reshaping berm breakwaters. Coast Eng. 104, 1–12. https://doi.org/10.1016/j.coastaleng.2015.06.003.

Moghim, M.N., Shafieefar, M., Tørum, A., Chegini, V., 2011. A new formula for the sea state and structural parameters influencing the stability of homogeneous reshaping berm breakwaters. Coast Eng. 58 (8), 706–721. https://doi.org/10.1016/j.coastaleng.2011.03.006.

PIANC, 2003. State-of-the-art of Designing and Constructing Berm Breakwaters (Report of Working Group 40). International Navigation Association, Brussels, Belgium.

Shafieefar, M., Shekari, M.R., Hofland, B., 2020. Influence of toe berm geometry on stability of reshaping berm breakwaters. Coast Eng., 103636

Shekari, M.R., Shafieefar, M., 2013. An experimental study on the reshaping of berm breakwaters under irregular wave attacks. Appl. Ocean Res. 42, 16–23. https://doi.org/10.1016/j.apor.2013.03.007.

Sigurdarson, S., Van der Meer, J., 2013. Design of berm breakwaters, recession, overtopping and reflection Coasts. In: Marine Structures and Breakwaters 2013. Edinburgh, Scotland. https://doi.org/10.13140/2.1.1433.4723.

Sigurdarson, S., van der Meer, J., Tørum, A., Tomasicchio, G., 2008. Berm recession of the icelandic-type berm breakwater. https://doi.org/10.1142/9789814277426_0274.

Sigurdarson, S., Viggosson, G., Benediktsson, S., Einarsson, S., Smarason, O.B., 1999. Berm breakwaters, fifteen years experience. Coast Eng. 1998, 1407–1420. https://doi.org/10.1061/9780784404119.104.

Sveinbjörnsson, P.I., 2008. Stability of Icelandic Type Berm Breakwaters. Delft University of Technology, Faculty of Engineering and geosciences, Deåpartment of Hydraulic Engineering.

Tørum, A., 2007. Berm breakwaters revisited. Preliminary Internal Note, Department of Civil and Transportation Engineering. Norwegian University of Science and Technology, Trondheim, Norway.

Tørum, A., Kuhnen, F., Menze, A., 2003. On berm breakwaters. Stability, scour, overtopping. Coast Eng. 49 (3), 209–238. https://doi.org/10.1016/S0378-3839(03)00062-0.

Van der Meer, J., Sigurdarson, S., 2016. Design and Construction of Berm Breakwaters, 40. World Scientific Publishing Co. https://doi.org/10.1142/9936

Van der Meer, J.W., 1988. Rock slopes and gravel beaches under wave attack, p. 214. PhD thesis, Delft Hydraulics, The Netherlands.

van der Meer, J.W., Veldman, J.J., 1992. Singular points at berm breakwaters: scale effects, rear, round head and longshore transport. Coast Eng. 17 (3), 153–171. https://doi.org/10.1016/0378-3839(92)90049-Z.